ScieRxiv

NOT PEER-REVIEWED

Review

The precise synthesis of etched MOF nanomaterials and their applications in electrochemistry

Sitong Wang[1], Jiayi Fan[1], Sijin Li[1], Mohsen Shakouri[2], Rongmei Zhu[1]*

[1]School of Chemistry and Materials, Yangzhou University, Yangzhou 225002, Jiangsu, China.

[2]Canadian Light Source, University of Saskatchewan, Saskatoon, Saskatchewan S7N 2V3, Canada.

***Correspondence to:** Dr. Rongmei Zhu, School of Chemistry and Materials, Yangzhou University, Yangzhou 225002, Jiangsu, China. E-mail: rmzhu@yzu.edu.cn

Received: 08 May 2026 | Approved: 20 May 2026 | Online: 20 May 2026

Abstract

Metal-organic frameworks (MOFs) have garnered extensive utilization across chemical, biomedical, and energy-related disciplines owing to their exceptional specific surface area and tunable structural features. Nevertheless, the electrical conductivity and long-term durability of conventional MOF materials remain inadequate for many advanced applications. Etching approaches offer a promising route to generate additional defect sites and catalytic centers within MOF architectures and their derivatives, thereby significantly expanding their functionality in electrochemical systems. This review systematically elaborates on various etching techniques, encompassing hard- and soft-templating routes, metallic ion etching, and ligand exchange protocols. It further

DOI: 10.20517/scierxiv202605.0330.v1

highlights the performance of etched MOFs in electrocatalytic processes, supercapacitors, and battery technologies. Prospects for future development and prevailing challenges in the field of etched MOF materials are also critically discussed.

Keywords: Metal-organic framework, etching approach, electrolysis, energy storage

INTRODUCTION

The escalating global energy demand and the accelerating depletion of conventional fossil resources have precipitated severe environmental challenges. In response, the development of clean and renewable energy alternatives, such as solar, wind, tidal, and hydrogen energy, have become an imperative strategy to mitigate reliance on traditional carbon-based fuels[1]. Within this context, metal organic frameworks (MOFs) have emerged as a class of materials with significant potential for energy applications[2]. Comprising metal nodes interconnected by organic ligands through coordination bonds, MOFs represent a distinctive family of porous crystalline materials that have attracted considerable attention over the past twenty years[3-5]. In contrast to conventional porous solids, MOFs exhibit exceptional characteristics, including ultrahigh surface areas, tunable pore geometries, and synthetic sustainability. These attributes render them highly promising for a diverse range of applications, spanning gas adsorption and storage, molecular sensing, drug delivery, and catalytic processes[6].

The synthesis and properties of MOFs are strongly influenced by the selection of metal ions, organic linkers, and functional modifiers[7,8]. Notably, even identical precursor combinations can yield distinct structural configurations and material characteristics, underscoring the critical role of synthetic control[9]. Variations in synthesis methods and reaction conditions further modulate morphology, crystallinity[10-12], and porosity, thereby directly determining the functional performance of the resulting materials[13]. Despite their advantages in porosity and tailorability, MOFs often suffer from intrinsic limitations such as poor electrical conductivity[14], limited chemical resilience, particularly under acidic conditions due to the labile nature of coordination bonds and

insufficient mechanical robustness[15,16]. These shortcomings significantly restrict their applicability, especially in electrochemical systems[17]. Moreover, the predominantly microporous nature (pores < 2 nm) of conventional MOFs imposes diffusion constraints, narrowing their utility in composites and processes requiring rapid mass transport[18,19].

As a result, strategies such as composite formation, ligand exchange, and etching have been developed[20,21]. Among these, etching techniques have proven particularly effective in engineering hierarchical porosities and exposing abundant active sites while largely preserving the innate high surface area and structural integrity[22]. The resulting etched MOFs exhibit significantly enhanced functionality, opening new avenues for advanced applications[22].

Recent studies highlight the considerable potential of chemical etching in modulating both the functionality and microstructure of MOFs[23,24]. This review comprehensively examines etching strategies aimed at enhancing the electrochemical performance of MOFs[25]. These approaches can be categorized according to the use and nature of templates[26,27], such as hard or soft templates, or by the targeting of specific components[14], including metal nodes and organic ligands[28]. We critically evaluate the merits and limitations of each etching strategy, systematically summarize recent breakthroughs in the electrochemical applications of etched MOFs [Figure 1], and offer perspectives on future research directions and challenges in this evolving field[29].

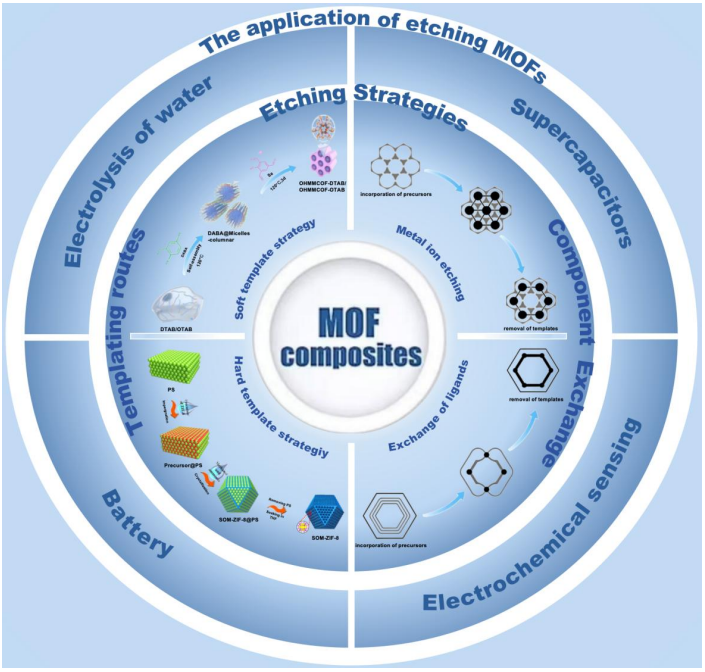

Figure 1. Summary of Etching Strategies.

METHODS OF ETCHING MOFS

In recent years, numerous synthesis strategies for MOFs have been developed, including conventional solvothermal routes, template-assisted growth, and ultrasound-assisted preparation[30,31]. Despite these advances, the inherently narrow pore size distribution of many MOFs often restricts their efficiency in energy storage applications[32,33]. Rational modulation of the pore architecture represents a critical pathway to overcome this limitation[34]. Chemical etching, which operates through selective cleavage of coordination bonds between metal ions and organic ligands, has emerged as an effective means to tailor pore characteristics[35]. Precise control over etching parameters is essential to achieving desired structural properties[36], including porosity, morphology, crystal facet exposure, and chemical composition[37]. This section outlines three principal etching approaches: template method, metal ion exchange and ligand exchange[38,39].

Template method

Based on the nature of the templating materials, template-based synthesis strategies can be categorized into hard-templating and soft-templating approaches[40,41]. An ideal template should combine ease of preparation with controlled etchability, thereby

enabling the precise preservation of the desired MOF architectures and morphological features.

Hard template strategies

Hard templates, including SiO_2, metals, and polymers, typically exhibit well-defined and tunable geometries that facilitate the formation of core-shell architectures. Subsequent removal of the core template allows the preservation of the shell's original morphology[42]. The fabrication of hollow MOFs via hard-templating generally involves three key steps: first, synthesis of a template with specific shape and dimensions; second, controlled growth of the MOF shell over the template surface; and finally, removal of the core to yield hollow structures[43]. For instance, Wang *et al.* constructed nitrogen-doped carbon hollow microtubules (denoted as N-GCT) using ZnO nanorods as a sacrificial template in a ZnO@ZIF-8 system [Figure 2a][41]. Their study revealed that the shell thickness could be precisely modulated by varying the reaction time or temperature. After etching with KOH, the resulting N-GCT retained a well-defined hollow architecture without structural collapse, and exhibited high specific surface area and pore volume[25], resulting of enhanced performance as a cathode material in lithium-sulfur batteries[29,44].

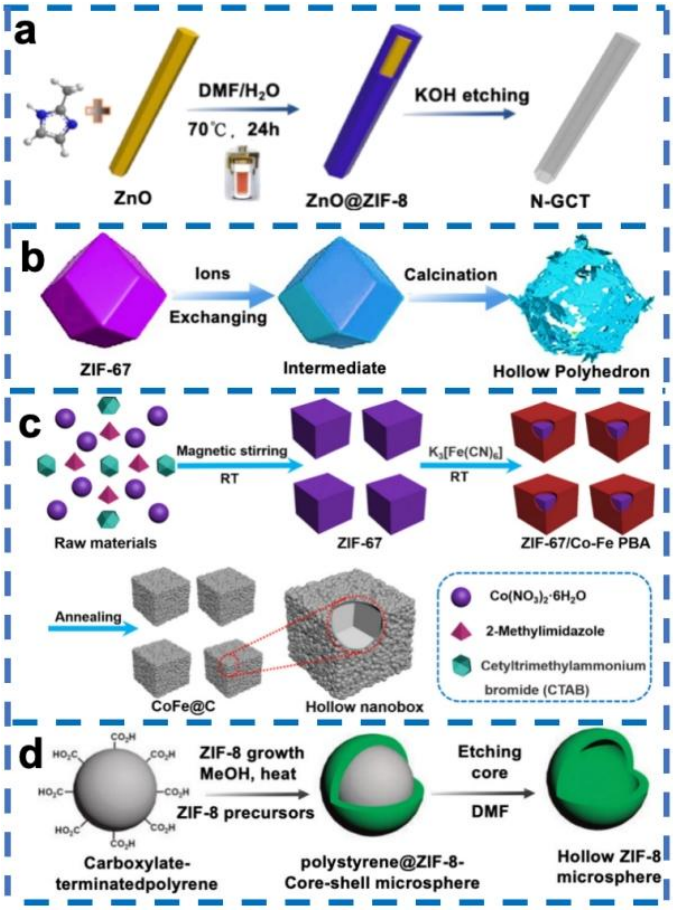

Figure 2. Schematic representation of the preparation of (a) N-GCT; Reprinted with permission. Copyright 2022, Springer Nature; (b) hollow CeO_2/Co_3O_4 polyhedrons; Reprinted with permission.Copyright 2021, Elsevier; (c) hollow CoFe@C nano-boxes; Reprinted with permission. Copyright 2021, Elsevier; (d) hollow ZIF-8 microspheres; Reprinted with permission. Copyright 2012, Royal society of chemistry.

Beyond conventional metal oxide templates, MOFs have been employed as sacrificial templates to fabricate hollow polyhedral architectures[45]. For instance, Zhang *et al.* synthesized hollow CeO_2/Co_3O_4 polyhedra by utilizing ZIF-67 as a precursor template [Figure 2b]. Through a surface ion-exchange process followed by high-temperature calcination to remove the internal template, a hollow polyhedral morphology with an average size of 200 nm was achieved[46,47]. When applied as a cathode catalyst in Li-O_2 batteries, the CeO_2/Co_3O_4 polyhedron significantly enhances the electrolyte-cathode interfacial contact and shortens the diffusion pathway for both lithium ions and oxygen, thereby improving the reaction kinetics[48]. In another approach, Wei *et al.* constructed

hollow CoFe@C nanoboxes using cubic ZIF-67 as a hard template[49] shown in Figure 2c. The surfactant cetyltrimethylammonium bromide (CTAB) was critical in selectively inhibiting the growth of the (100) crystal facets, promoting the formation of a well-defined cubic architecture[50]. This enabled the subsequent formation of ZIF-67/Co-Fe Prussian blue analogue (PBA) multilayer nanoboxes[11]. Family, during annealing, the ZIF-67 template was etched away, resulting in hollow nanoboxes with maintained structural integrity.

Among various hard-template options, polystyrene (PS) spheres are widely utilized for constructing hollow MOFs and MOF-based composites owing to their mild synthesis and removal conditions[51]. Oh *et al.* pioneered the use of PS templates to fabricate hollow ZIF-8 microspheres via a distributed solvothermal reaction[52] as shown in Figure 2d. Carboxyl groups on the PS surface facilitate zinc ion coordination, promoting heterogeneous nucleation and growth of ZIF-8 on the template. Subsequent immersion in selectively removes the PS core, yielding intact hollow microspheres. By precisely controlling the growth cycles, the ZIF-8 shell thickness can be finely tuned, enabling optimization of the material's physicochemical and functional properties[53]. Furthermore, the versatility of PS templates allows the engineering of more complex architectures，such as hollow double-shell MOF structures through iterative templating strategies.

Despite its utility in fabricating hollow MOFs, the hard-template method encounters several challenges during the etching process. These include difficulty in completely removing the template, limited structural stability of the resulting MOFs, imprecise control over pore size distribution, and overall procedural complexity[54]. In contrast, soft-templating strategies offer notable advantages: milder template removal conditions, finer regulation of pore architecture, improved structural integrity of the MOFs, and a more streamlined synthesis process[55] These characteristics make soft-template etching particularly suitable for constructing MOFs with hierarchical porosity, well-defined hollow morphologies, and tailored functionality[21,56].

Soft template strategy

Surfactants, by virtue of their amphiphilic nature, self-assemble into micelles or vesicles in solution, serving as soft templates to direct the formation of tailored nanostructures[57]. Surfactants like sodium dodecyl sulfate (SDS) and alkyltrimethylammonium bromide (C_nTAB) are particularly effective for crafting hollow MOFs through etching strategies[58,59]. Electrostatic interactions and hydrogen bonding facilitate the crystallization of MOFs on the surfactant surfaces, while morphological control can be achieved by tuning surfactant concentration, reaction temperature, and pH[60].

For instance, Lei's group fabricated hollow ZIF-8 nanospheres using anionic SDS micelles as templates[61]. The negatively charged SDS surface attracts zinc cations, promoting the subsequent coordination with 2-methylimidazole and leading to the controlled growth of a ZIF-8 shell around the micelle[62]. Washing with deionized water removes the SDS template, yielding hollow ZIF-8 architectures as presented in Figure 3a. Beyond anionic systems, cationic soft templates such as C_nTAB vesicles have also been employed. Zhang *et al.* demonstrated that upon mixing C_nTAB with $Co(NO_3)_2$ and HmIM in aqueous solution, negatively charged [Co-complex]$^-$ species adsorb onto the cationic vesicle surface, providing nucleation sites for ZIF-67 crystallization[63]. Subsequent washing with DMF and methanol etches away the soft tmplate, resulting in hollow ZIF-67 particles with uniform structural integrity[64,65] [Figure 3b].

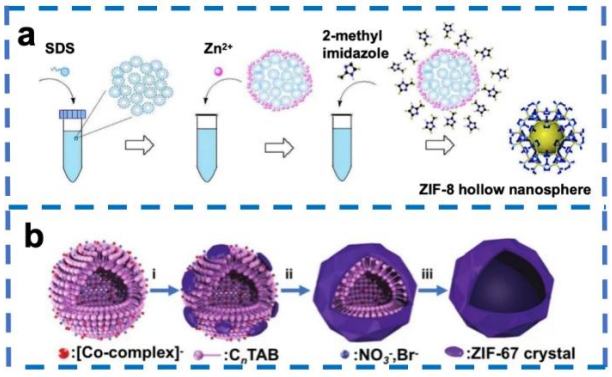

Figure 3. (a) Preparation of ZIF-8 hollow nanospheres; Reprinted with permission. Copyright 2015, Elsevier; (b) Simplified illustration of the growth mechanism of ZIF-67 hollow structure; Reprinted with permission. Copyright 2016, Wiley.

Exchange of metal ions

A wide variety of MOFs with diverse compositions and structural features have been extensively investigated. Key strategies for tailoring MOF architectures include central metal ion exchange, ligand etching and substitution, defect engineering, template-guided assembly, and ligand functionalization. While extending the length of organic linkers can facilitate the formation of mesopores of varying sizes, it often compromises the framework stability due to reduced coordination connectivity[66]. Among these approaches, etching and exchanging central metal ions represent one of the most straightforward routes to structural modification[67]. These processes not only alter the chemical composition but also enable precise control over morphology and crystalline orientation. Commonly employed metal ion etching techniques involve proton acid etching and competitive metal ion displacement, which typically target specific crystal facets or sites to create enlarged mesopores or customized morphological features[68,69].

Acid etching serves as a highly effective route for constructing hierarchical porous MOF architectures. By selectively cleaving coordination bonds between metal nodes and organic ligands using proton acids, this method enables precise control over MOFs' morphology[70], facilitating the creation of hollow and highly porous structures. Liu *et al.* developed a synergistic protection etching strategy to fabricate hollow ZIF-67 polyhedra and carbon nanocages (Co@NCNs)[71] displayed in Figure 4a, circumventing the limitations of conventional sacrificial templates and strong etchants[72]. Tannic acid (TA), rich in hydroxyl groups, was coated on ZIF-67 surfaces. Protons released from TA diffused inward through pores, selectively breaking Co-N bonds and inducing core-selective etching, with shell thickness finely adjustable via etching duration[73]. Huo's group demonstrated multi-shell hollow MIL-101(Cr) with single-crystal shells through stepwise crystal growth and acetic acid etching[74] [Figure 4b]. The differential stability between outer and inner layers allowed selective etching, with cavity size and shell thickness modulated by etching time and reactant concentration.

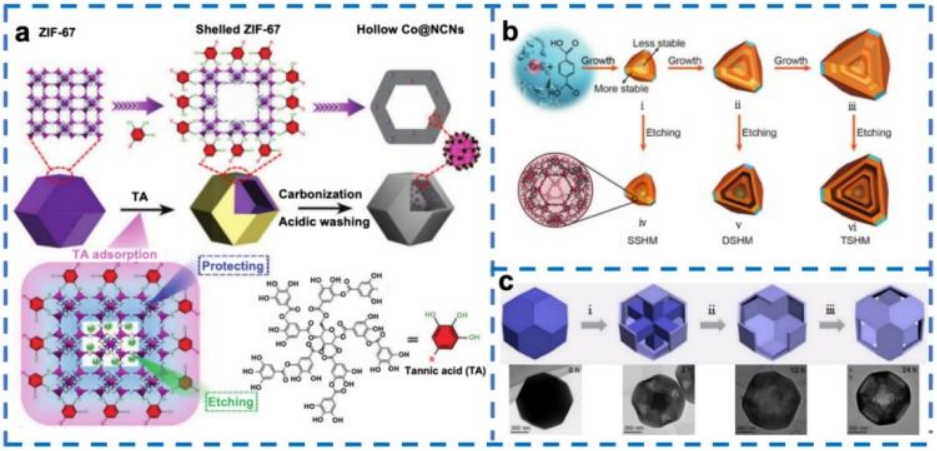

Figure 4. The schematic illustration for the synthetic procedure of (a) hollow Co@NCNs; Reprinted with permission. Copyright 2021, Wiley; (b) single-, double-, and triple-shelled hollow MIL-101; Reprinted with permission. Copyright 2017, Wiley; (c) tZIF-67 hollow nano-frame and the corresponding TEM images; Reprinted with permission. Copyright 2021, Wiley.

The Ting group utilized phosphoric acid to selectively etch the metastable HKUST-1, generating a defect-rich porous copper-based MOF with hexagonal macroporosity while preserving crystallinity[75]. Their experiments confirmed etching dependence on both time and acid concentration. As shown in Figure 4c, Yamauchi *et al.* employed cyanuric acid (CA) to anisotropically etch ZIF-67 truncated rhombic dodecahedra. CA preferentially passivated the (100) facets, enabling inward excavation of the six equivalent crystal planes, ultimately yielding well-defined hollow nanoframes[76].

Layered double hydroxides (LDHs) belong to a class of anionic layered materials characterized by brucite-like sheets in which metal cations occupy octahedral sites coordinated by hydroxyl groups[77]. Owing to their tunable chemical composition, ion-exchange capability, high intrinsic stability, and rich redox properties, LDHs exhibit outstanding performance across various application[78]. Recently, metal ion etching has been widely adopted for synthesizing LDHs with hierarchical structures from MOF precursors, significantly enhancing the electrochemical utility of MOF-derived materials[79,80]. For example, Qiu *et al.* constructed bimetallic NiCo-LDH polyhedra

through Co^{2+} and Ni^{2+} etching of ZIF-67[81]. As displayed in, the bimetallic system promotes the formation of numerous ultra-thin, vertically aligned LDH nanosheets assembled into hollow polyhedral superstructures in contrast to monometallic Co-LDH. This unique configuration maximizes interfacial exposure and facilitates guest-host interactions, thereby enhancing electrochemical activity[82]. Similarly, Li *et al.* converted Co-ZIF-L into CoNi-LDH with tunable morphologies and properties via a multi-step ion-etching approach[83]. The Co-ZIF-L was first etched with Co^{2+} in a DMF-ethanol solution, followed by further Ni^{2+}-assisted etching, yielding a material labeled CoNi-1 that demonstrated superior electrochemical performance[84,85].

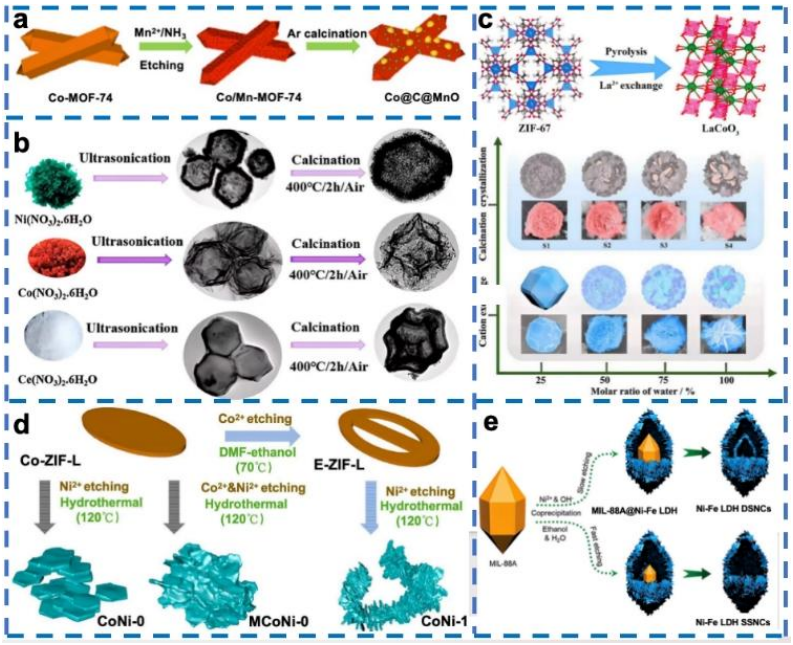

Figure 5. Schematic illustration of preparing (a) hierarchical Co@C@MnO nanorods; Reprinted with permission. Copyright 2021, Elsevier; (b) Hollow Cages Ni/Co_3O_4, Co_3O_4-30, and Ce/Co_3O_4; Reprinted with permission Copyright 2021, Elsevier; (c) Schematic illustration of La^{3+} etching effect on ZIF-67 and their corresponding pyrolysis products, Reprinted with permission. Copyright 2020, Elsevier; (d) CoNi-LDH from Co-ZIF-L; Reprinted with permission. Copyright 2024, Elsevier; (e) Ni-Fe LDH nanocages with tunable shells. Copyright 2021, Wiley.

Furthermore, the shell architecture of hollow LDHs, including shell number and

hierarchy, can be precisely tailored by modulating etching conditions[86]. As demonstrated by Gao's group, adjusting the ethanol-to-water ratio during etching allows fine control over reaction kinetics[87]. With higher ethanol content, etching is slowed, leading to the formation of double-shelled Ni-Fe LDH nanocages (DSNCs), as illustrated in Figure 5e. In contrast, aqueous-rich conditions favor single-shelled structures[88,89].

Building upon the complementary strengths of proton acid etching, which enables hollow structure formation and transition metal ion etching that allows crystal structure regulation, the integration of both strategies offers a powerful route for fabricating anisotropic materials with finely tunable composition and architecture[90]. Liu *et al.* demonstrated this synergistic approach by simultaneously employing transition metal and protic acid etching to synthesize hollow carbon polyhedral. In their method, Ni^{2+} ions first etched ZIF-67 to form a NiCo@LDH intermediate, which was subsequently treated with boric acid (H_3BO_3) to selectively etch the framework, resulting in well-defined hollow structures with maintained polyhedral morphology[91].

Exchange of ligands

*Beyond metal i*on etching, etching and exchange represent another effective approach for structural and compositional modulation of MOFs[92]. This strategy readily yields hollow architectures and novel chemical functionalities. Alkaline agents or strongly coordinating ligands are typically employed as etchants to selectively remove or replace original linkers, thereby creating porous frameworks or inducing phase transformations[93].

For example, Li *et al.* demonstrated alkaline etching of a copper-based MOF (Cu-MOF-74) to synthesize hollow copper sulfides with tunable morphologies. As illustrated in Figure 5a, sequential treatment with KOH and Na_2S first induced a pseudo-crystalline transformation under alkaline conditions, progressively evolving the initial rod-like morphology into cubic (30 min) and dodecahedral (180 min)

intermediates. Subsequent sulfidation yielded the corresponding hollow sulfide derivatives[94]. In a related study, Zhang *et al.* utilized $NH_3 \cdot H_2O$ as an alkaline etchant to convert solid Co-Co Prussian blue analogue (PBA) cubes into hollow Cu-$CoSe_2$ nano-frames (NFCs) in a water-ethanol mixture. Hydroxide ions generated from ammonia cleavage selectively removed the inner $Co(CN)_6^{3-}$ ligands, resulting in structurally defined hollow frameworks[95]. Alternatively, Liu *et al.* introduced a dry etching approach using thiourea as a sulfurizing agent to convert MIL-88A into Fe_7S_8/C composites. At 650 °C, thiourea decomposition releases H_2S, which serves as a gaseous etchant enabling sulfide formation through reaction with Fe^{3+} nodes[96].

Zhang *et al.* further developed an ammonia-assisted in situ cation exchange method to fabricate dodecagonal N-doped carbon nanosheets (Pd-e-NiCo-PBA-C). Unlike conventional cubic hollow structures, this unique skeletal framework resulted from anisotropic etching initiated at the vertices of the precursor cube, evolving progressively into a cage-like architecture and ultimately a hollow morphology, exhibiting exceptional electrocatalytic performance in water splitting[97].

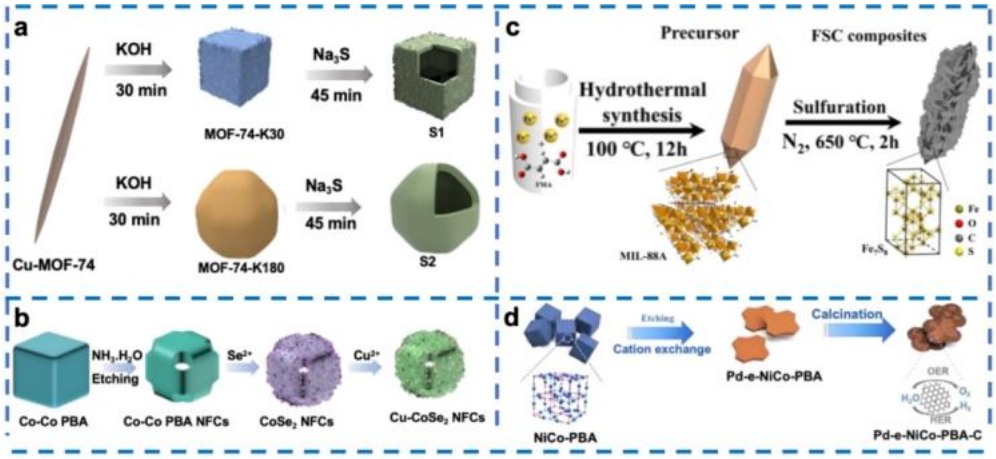

Figure 6. Schematic illustration of preparing (a) hollow structures by etching Cu-MOF-74; Reprinted with permission. Copyright 2022, Elsevier; (b) Cu-$CoSe_2$ NFCs; Reprinted with permission. Copyright 2022, Elsevier; (c) Fe_7S_8/C composites; Reprinted with permission. Copyright 2021, Elsevier; (d) Pd-e-NiCo-PBA-C; Reprinted with permission. Copyright 2021, Wiley.

ETCHING MOF-DERIVED HETEROSTRUCTURES

The morphology of MOFs can be categorized into one-dimensional forms such as nanorods and nanobelts, two-dimensional nanosheets, and three-dimensional architectures including nanoflowers and polyhedra[98]. Through etching strategies, both MOFs and their derivatives can be engineered into advanced configurations, such as hollow, core-shell, and ring-shaped structures that extend beyond their original frameworks. These modified materials not only retain the inherent structural advantages of MOFs but also facilitate enhanced charge transfer across multi-component interfaces, significantly boosting electrochemical performance[99]. This section will focus particularly on two prominent etched architectures: core-shell and hollow structures.

Core-shell structure

Core-shell nanostructures constitute a significant class of nanomaterials characterized by a distinct core enveloped by a surrounding shell[100]. Broadly speaking, they comprise ordered architectures formed through the encapsulation of one nanomaterial by another via chemical bonds or physical interactions, encompassing both conventional core-shell configurations and yolk-shell structures that incorporate an interstitial void between core and shell[101].

In the context of MOF-based core-shell systems, structural design has evolved from relatively simple forms to increasingly complex architectures. The shell serves a critical protective role, shielding the core from the external environment and providing a confined space that enhances reaction stability. When the shell is composed of porous MOFs, it further facilitates molecular transport by offering additional pore channels, shortening diffusion pathways, promoting electrolyte infiltration, especially in hollow configurations and enhancing charge and mass transfer kinetics[102,103]. Moreover, the synergistic interplay between core and shell components enables the integration of multifunctional properties, substantially broadening the application potential of these materials across catalytic, energy storage, sensing, and biomedical fields[104].

Single-layer core-shell structures are commonly fabricated via self-templating methods, which enable precise control over dimensions and morphological uniformity[105]. In contrast to conventional hard- or soft-templating approaches, self-templating not ensures well-defined core-shell architectures but also allows tailored regulation over MOF composite properties. Among various synthetic routes, the one-pot method represents a straightforward and efficient strategy, wherein metal precursors and organic ligands are simultaneously introduced into a reaction system to achieve in situ core encapsulation and shell formation with narrow size distribution[106,107]. For instance, Wang and Xu constructed a core-shell system comprising semiconductor CdS nanoparticles as the core and ZIF-8 as the shell using a two-step approach [Figure 7a][108]. Initially, polyvinylpyrrolidone (PVP)-stabilized CdS NPs were synthesized, followed by controlled growth of a ZIF-8 shell onto the CdS surface. By varying the concentration of the 2-methylimidazole precursor, the thickness of the ZIF-8 shell could be precisely tuned from 102 ± 5.4 nm down to 13.6 ± 2.5 nm[109].

In a separate study, Chen *et al.* developed a layer-by-layer epitaxial growth method to fabricate Fe_3O_4@UiO-66-NH_2 core-shell structures shown in Figure 7b. Magnetic Fe_3O_4 nanoparticles were sequentially immersed in ethanolic solutions containing the zirconium cluster precursor $Zr_6O_4(OH)_4^{12+}$ and the organic linker 2-aminoterephthalic acid, with magnetic separation after each step, to achieve uniform MOF encapsulation[110]. Diverging from these approaches, Prof. Yu's group designed a yolk-shell nanoreactor using MIL-101 as the core and mesoporous silica ($mSiO_2$) as the shell, followed by a water etching step to create interstitial voids[111] [Figure 7c]. In contrast to conventional chemical etching, water etching offers an environmentally benign and cost-effective route for generating highly porous yolk-shell structures without aggressive reagents.

From a structural perspective, MOF-derived core-shell architectures can be classified into two primary categories: single-shell and multi-shell systems. Unlike their

single-shell counterparts, multi-shell heterostructures incorporate multiple concentric or hierarchical layers, offering enhanced compositional complexity and tailored functionality[112]. These sophisticated architectures can be synthesized through self-templating strategies, often coupled with selective etching or ion-exchange processes. For example, Shen *et al.* fabricated hollow spherical structures starting from solid NiCo metal glycerate spheres[113]. Through hydrothermal anion exchange, they sequentially transformed these precursors into core-shell, yolk-shell, and ball-in-ball hollow spheres, demonstrating the versatility of ion-based transformation pathways [Figure 7d].

Alternatively, carbon-rich MOFs prepared via solvothermal methods exhibit exceptional metal cation permeability, enabling the construction of multi-shell hollow structures through post-synthetic modification. Guan *et al.* illustrated this approach by first synthesizing Mn-Co coordination polymer spheres through solvothermal reaction of Mn^{2+} and Co^{2+} with isophthalic acid (H_2IPA)[114]. The resulting precursor was subsequently calcined to form multi-shell bimetallic oxide particles and then phosphatized using NaH_2PO_2 to yield multi-shell Mn-Co oxyphosphide, as depicted in Figure 7e.

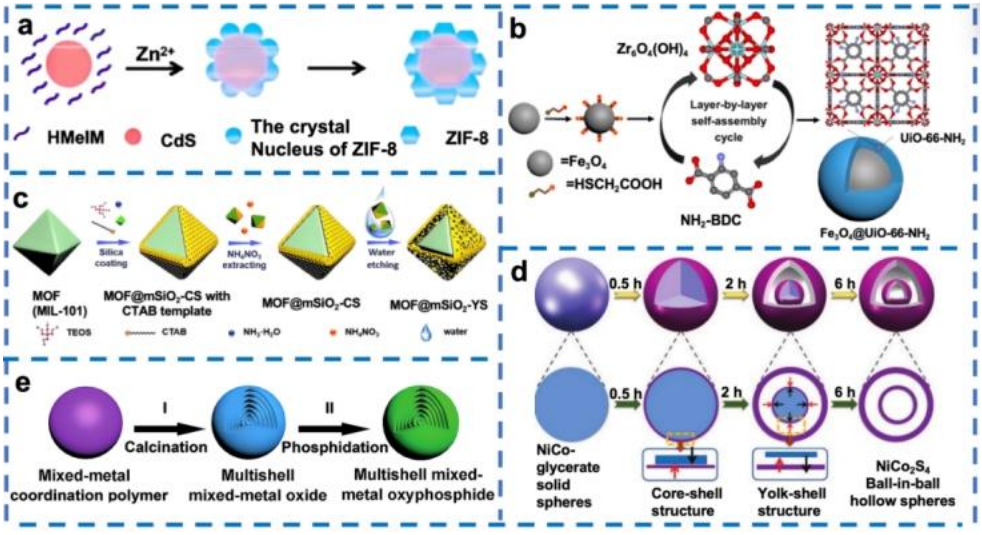

Figure 7 Schematic preparation of (a) CdS@ZIF-8 core-shell structure; Reprinted with permission. Copyright 2016, Springer Nature; (b) Fe_3O_4@UiO-66-NH_2 core-shell

structure; Reprinted with permission. Copyright 2019, American Chemical Society; (c) Yolk-shell MOF@mSiO$_2$-YS nanoreactors; Reprinted with permission. Copyright 2020, Elsevier; (d) NiCo$_2$S$_4$ ball-in-ball hollow spheres; Reprinted with permission. Copyright 2015, Springer Nature; (e) multishell mixed-metal oxyphosphide particle; Reprinted with permission. Copyright 2024, John Wiley and Sons.

Hollow structure

Hollow nanostructured materials possess a range of advantageous properties, including high specific surface area for enhanced mass diffusion, abundant exposed active sites adaptable to diverse applications, and substantial internal void space enabling high loading capacity[115]. Etched MOFs with hollow architectures further benefit from tunable surface chemistry, enlarged pore size, and elevated surface area[116]. Notably, their hollow morphology facilitates rapid electrolyte penetration and efficient gas release compared to solid counterparts, contributing to their widespread use and high performance across numerous applications.

Two primary strategies are employed for fabricating hollow MOFs and their derivatives: template-assisted and post-processing methods. In the template-assisted approach, hollow structures are formed during MOF synthesis by growing the framework around a sacrificial template, such as silica or polystyrene spheres, followed by template removal. For instance, Prof. Jiang synthesized hollow porous carbon (HPC) by pyrolyzing ZIF-8 grown on PS templates, resulting in a porous shell with high surface area that significantly enhances catalytic efficiency[117] [Figure 8a]. In contrast, Lou and colleagues adopted a post-processing strategy as shown in Figure 8b, constructing hollow ZIF-67 prismatic nanostructures through rapid ion exchange using Co(CH$_3$COO)$_2$(OH)$_3$ nanoprisms as sacrificial templates[118]. Subsequent sulfidation transformed these into hollow CoS$_2$ particles that retained the prismatic morphology. The formation of the hollow interior is driven by the outward diffusion of Co^{2+} ions from the precursor nanoprisms and the inward migration of organic ligands, leading to the oriented growth of ZIF-67 polyhedra on the template surface and ultimately yielding

well-defined hollow structures[119].

Subtle variations in reaction conditions can significantly influence the final morphology and composition of products. Li's group highlighted the role of solvent mediation in shaping bimetallic ZIF structures, demonstrating that hollow Co-ZIF phases can be transformed from ZIF-67 seeds in methanol through Co^{2+} assistance[120] [Figure 8c upper]. This strategy was extended to the synthesis of hollow Zn/Co-ZIF, where a core-shell ZIF-67@ZIF-8 intermediate underwent Zn^{2+}-mediated etching. The gradual decrease in Zn concentration indicated selective etching of the inner ZIF-8 shell, resulting in a hollow rhombohedral dodecahedron with a Co-rich ZIF-67 core enclosed by a Zn-containing ZIF-8 shell [Figure 8c below].

Hollow layered double hydroxide (LDH) nanostructures derived from MOFs have also emerged as promising materials for catalysis and energy storage. Prof. Mirsaidov's team utilized liquid-phase transmission electron microscopy to visualize the transformation of ZIF-8 templates, both nanocubes and rhombic dodecahedra, into hollow LDH nanocages that is shown in Figure 8d. Their work revealed that the kinetics of ZIF-8 etching and LDH nucleation must be carefully balanced to achieve well-defined hollow structures, emphasizing the critical role of reaction rate matching in structural evolution[121].

The post-processing approach involves the formation of hollow structures through the modification of pre-synthesized MOFs. As an effective strategy, etching eliminates the need for template removal and offers distinct advantages over hard-templating methods, which often rely on particle agglomeration[122]. In contrast, etching can be applied to single-crystalline MOFs, enabling precise control over cavity dimensions and shell thickness by modulating the etching extent. To achieve well-defined hollow structures via chemical etching, the integrity of the MOF shell must be maintained throughout the process[123]. Tannic acid (TA) has been widely employed for this purpose, owing to its strong surface adhesion and metal-coordination capabilities, as noted in Section 2.2[124]. During etching, TA forms a protective layer on the MOF surface, preventing structural

collapse, while the released protons diffuse inward to selectively remove the core. The molecular size of the etchant is critical: appropriately sized agents ensure uniform surface coverage and controlled etching, whereas mismatched sizes may lead to irregular pore formation or framework degradation[125]. Formic acid, for instance, can modify MOF surfaces without altering their crystalline phase. It modulates the distribution and accessibility of unsaturated metal sites, thereby enhancing porosity, specific surface area, and charge transfer efficiency, which collectively improve electrochemical and catalytic performance[126].

In addition to acid etching, metal ion etching was discussed in Section 2.2. Another notable method is oxidative linker cleavage within single-crystalline MOFs, introduced by Luo *et al.*[127]. As shown in Figure 8e, treatment of UiO-66-$(OH)_2$@UiO-66-Br with HNO_3 required 24 h to achieve complete hollowing. In contrast, when treated with much stronger oxidants (SO_4^- and •OH), the hollow structure was formed within just 1.5 h. This strategy also facilitates the dispersion of Pd nanoparticles within the MOF without aggregation, significantly boosting catalytic activity[128].

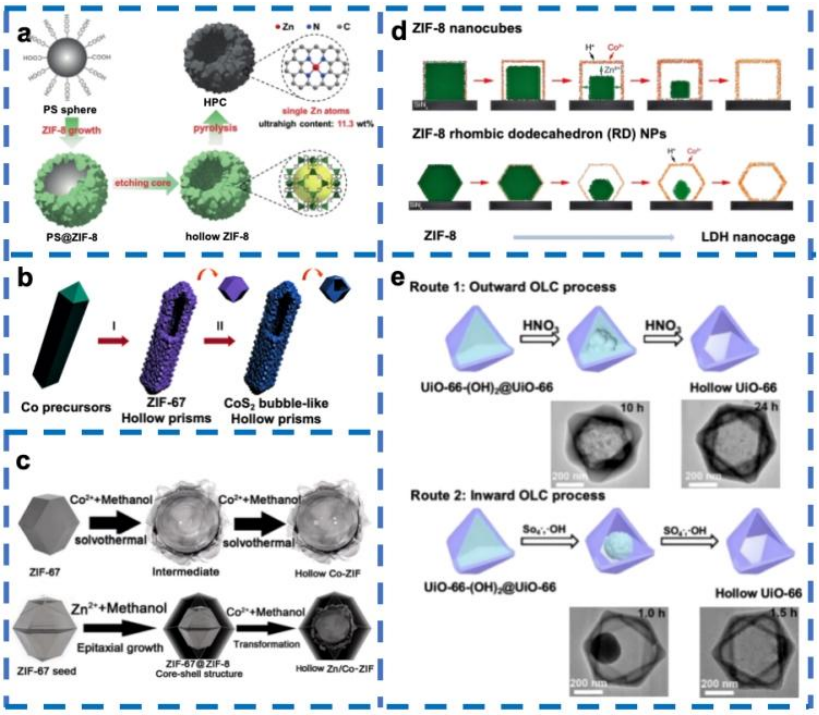

Figure 8. Schematic illustration showing (a) the preparation process of the HPC; Reprinted with permission. Copyright 2019, John Wiley and Sons; (b) the formation of CoS_2 nanobubble hollow prisms; Reprinted with permission. Copyright 2016, John Wiley and Sons; (c) the structural evolution of ZIF-67; Reprinted with permission. Copyright 2015, John Wiley and Sons; (d) the conversion of ZIF-8 into LDH nanocages; Reprinted with permission. Copyright 2021, American Chemical Society; (e) the two OLC processes; Reprinted with permission. Copyright 2019, American Chemical Society.

Undoubtedly, while a variety of heterostructures can be derived from MOFs through etching, core-shell and hollow configurations remain among the most representative and widely studied[129]. These two architectures offer distinct advantages: both significantly enhance the accessibility and exposure of active sites. Furthermore, the combination of intrinsic microporosity from the MOF framework and newly created mesoporosity from etching synergistically facilitates efficient mass transport within the structure[130]. This hierarchical porosity markedly improves ion diffusion and charge transfer, contributing substantially to enhanced electrochemical performance.

THE APPLICATION OF ETCHING MOFS

Electrolysis of water

Electrocatalytic water splitting is a promising method for converting electrical energy into chemical energy stored in hydrogen, offering a sustainable pathway for hydrogen production. During this process, the hydrogen evolution reaction (HER) takes place at the cathode, involving a two-electron transfer process that leads to the formation of H-H bonds[131]. Simultaneously, the oxygen evolution reaction (OER) occurs at the anode, comprising a complex multi-step mechanism involving O-H bond cleavage and O-O bond formation through proton-coupled electron transfers[132]. The intricate nature of OER results in inherently slow reaction kinetics, necessitating high overpotentials that limit the overall efficiency of water splitting and reduce the rate of oxygen generation.

As a result, the OER half-reaction is widely regarded as the bottleneck in electrocatalytic water splitting[133].

Phosphides exhibit remarkable properties such as high electrical conductivity, favorable electronic structure, and strong corrosion resistance, making them highly suitable for electrocatalytic applications. Specifically, cobalt phosphide (CoP) demonstrates high activity towards OER, attributed to the strong adsorption of oxygen intermediates on positively charged cobalt sites and facilitated O_2desorption by negatively charged phosphorus[134]. Lou's research group developed carbon-doped metal phosphide nanocubes derived from ZIF-67 to enhance OER performance. Initially, ZIF-67 nanocubes were synthesized via a surface-mediated method, then transformed into Ni-Co LDH through etching, and finally converted into Ni-Co mixed metal phosphide (NiCoP and NiCoP/C) through phosphorylation using NaH_2PO_2 [Figure 9a][135]. Among these, the hollow NiCoP/C nanoboxes achieved an overpotential of 330 mV at 10 mA cm^{-2} [Figure 9b], leveraging both the inherited high surface area and improved electrical conductivity from the MOF-derived hollow structure. These findings underscore the importance of morphological control in optimizing nanomaterial performance.

In our work, we synthesized high-valence metal-doped hollow CoP nanocubes through selective etching and ion exchange. By using xylenol orange solution to selectively etch the (211) crystal planes of truncated dodecahedral ZIF-67, where Co-N bonds are densely distributed, we obtained uniquely structured hollow intermediates[136]. Subsequent Hf^{4+} doping and phosphorylation yielded hollow Hf-doped CoP, which exhibited excellent OER performance with an overpotential as low as 292 mV at 10 mA cm^{-2} [Figure 9c and 9d]. Beyond conventional acid etching, we also developed an electrochemical Lewis acid co-etching and electrochemical adsorption doping method to incorporate larger-radius Hf ions into Co-MOF [Figure 9e]. This approach introduced beneficial defects and markedly enhanced OER kinetics, as evidenced by a significant reduction in the Tafel slope [Figure 9f]. This strategy of doping high-valence metals offers a novel pathway for designing high-performance electrocatalysts. Given the

challenging four-electron transfer processes in both OER and the oxygen reduction reaction (ORR), designing efficient and stable bifunctional catalysts is crucial for overall water splitting and regenerative fuel cells[137]. Using a triply layered ZIF precursor, we constructed yolk-shell hollow polyhedra (YHPs) embedded with ternary alloys and metal oxides through precisely controlled etching and pyrolysis [Figure 9g]. These YHP catalysts outperformed commercial benchmarks in both OER and ORR [Figures 9h], owing to the etching role of Lewis acid in forming yolk-shell configurations that provide abundant active sites and enhance mass and charge transfer[138].

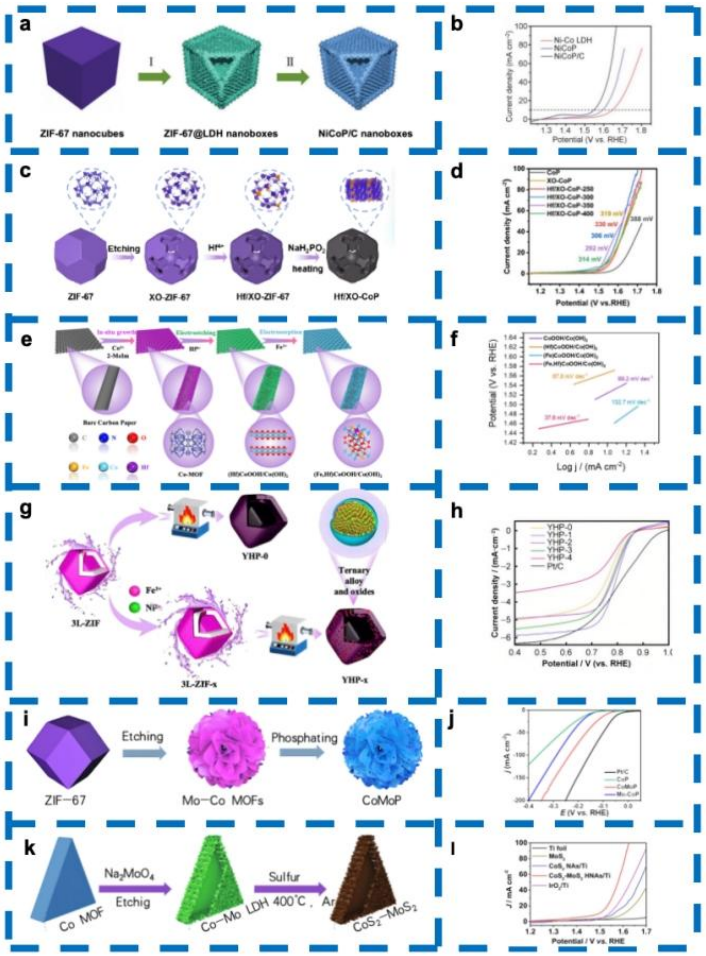

Figure 9. (a) Schematic illustration of the formation of NiCoP/C nano-boxes; (b) Polarization curves of Ni-Co LDH, NiCoP and NiCoP/C nano-boxes. Reprinted with permission. Copyright 2017, John Wiley and Sons; (c) Preparation diagram of the Hf/XO-CoP sample; (d) LSV polarization curves for the OER activity. Reprinted with permission. Copyright 2024, American Chemical Society; (e) Schematic illustration of

the synthetic process for (Fe,Hf)CoOOH/$Co(OH)_2$; (f) Tafel slops toward OER in 1 M KOH. Reprinted with permission. Copyright 2024, Royal society of chemistry; (g) Schematic illustration of synthetic procedure for YHP-x; (h) LSV curves toward ORR. Reprinted with permission. Copyright 2023, Elsevier; (i) Schematic illustration of the CoMoP synthesis; (k) OER Polarization curves; (j)HER polarization curves; Reprinted with permission. Copyright 2022, Elsevier; (k)Schematic illustration of the synthesis of CoS_2-MoS_2; (l)OER performance test curves.

As highlighted in previous sections, the development of bifunctional catalysts is critical for efficient electrocatalytic processes. While OER/ORR bifunctional catalysts have been widely explored, significant progress has also been made in designing HER/OER bifunctional catalysts for overall water splitting[139]. For instance, Wang *et al.* synthesized ultrathin CoMoP nanosheets through ion etching and phosphorylation of ZIF-67 [Figure 9i]. Treatment with ammonium molybdate induced both structural etching and partial substitution of Co^{3+} by Mo^{6+}, resulting in a porous, folded Mo-Co MOF intermediate[140]. Subsequent phosphorylation produced bimetallic phosphide nanosheets that exhibited exceptional activity and stability for both HER and OER [Figure 9j]. Similarly, Li and colleagues developed self-supported, hierarchically structured hollow CoS_2-MoS_2 heterojunction nanosheet arrays via controlled etching of a Co-MOF followed by in situ sulfurization shown in Figure 9k[141]. The resulting material featured abundant heterogeneous interfaces and optimized charge distribution, significantly promoting water dissociation and reaction kinetics. The two-dimensional hollow array architecture not only exposed numerous active sites but also facilitated electrolyte infiltration and rapid gas release[142]. The catalyst achieved low overpotentials of 82 mV for HER and 266 mV for OER at 10 mA cm^{-2}, respectively [Figure 9l].

Compared to their pristine counterparts, etched MOFs demonstrate superior and tunable functional properties. Etching serves as a versatile and efficient strategy for tailoring MOF-derived materials, enabling the creation of well-defined pore systems and the introduction of heteroatoms without phase segregation[143]. The incorporation of suitable

foreign metal species further modulates the electronic structure and enhances electrical conductivity, leading to improved electrocatalytic performance. Overall, the strategic optimization of both structure and composition is indispensable for advancing the efficacy of MOF-based electrocatalysts[144].

Supercapacitors

Supercapacitors represent a class of energy storage devices operating through Faradaic electrochemical processes, renowned for their long cycle life, rapid charge-discharge capability, and operational safety[145]. The capacitance of their electrode materials originates from surface-mediated processes, including electrochemical adsorption/desorption of ions and reversible redox reactions at the electrode-electrolyte interface[146].

Etched MOFs and their derivatives have emerged as high-performance electrode materials in supercapacitors, primarily due to their elevated specific surface area, abundant active sites, and tailored porosity resulting from etching, which collectively contribute to high specific capacitance[147]. When MOFs are etched with metal ions, they can be transformed into ultrathin bimetallic hydroxide nanosheets with hollow architectures[148]. The combination of layered morphology and hollow features accelerates ion diffusion, enabling efficient Faradaic redox reactions even at high current densities and thereby enhancing rate capability. For example, Zang *et al.* constructed polypyrrole nanotube (PNT)-supported ZIF-67-derived 3D nickel-cobalt LDH nanocages (PNT@NiCo-LDH) through solvothermal reaction and etching [Figure 10a]. The composite exhibited high electrical conductivity, robust cycling stability, and a notable specific capacitance of 1,448.2 F g^{-1} at 1 A g^{-1} [Figure 10b][149]. In another study, Ramachandran *et al.* synthesized NiCo-LDH by in situ etching of Ni-MOF templates under varied hydrolysis durations in the presence of $Co(NO_3)_2 \cdot 6H_2O$ [Figure 10c]. The etching time profoundly influenced the layered structure and surface area of the resulting LDH, facilitating rapid ion transport and achieving a maximum specific capacity of 1,272 C g^{-1} at 2 A g^{-1} [Figure 10d]. This approach offers a generalized strategy for

designing high-performance LDH-based energy materials[150]. Zhao *et al.* developed hollow and ultrathin Ni-Co sulfide nanosheet arrays on electrochemically activated carbon cloth (Ni-Co-S/ACC) shown in Figure 10e for flexible hybrid supercapacitors[151]. The material was derived from Co-MOF through ion exchange and sulfurization. The activated cloth substrate provided excellent flexibility and hydrophilicity, while the porous nanosheet array formed via a unique hydrolysis-etching process with $Ni(NO_3)_2$ and Na_2S, offered high surface area, abundant active sites, and shortened ion diffusion paths[152]. The Ni-Co-S/ACC electrode delivered an ultrahigh specific capacitance of 2,392 F g^{-1} at 1 A g^{-1} [Figure 10f] and maintained 80.3% capacitance retention at 20 A g^{-1}, underscoring its exceptional rate performance and practical potential.

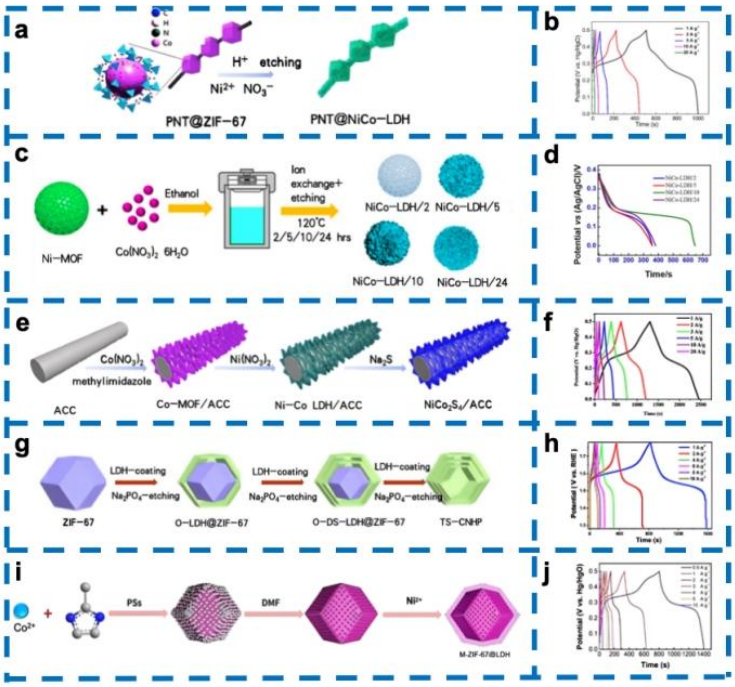

Figure 10. (a) Fabrication process of PNT@NiCo-LDH nano-cages; (b) GCD curves of PNT@NiCo-LDH nano-cages in the range of 1-20 A g^{-1}; Reprinted with permission. Copyright 2021, American Chemical Society. (c) Schematic diagram of NiCo-LDH synthesis; (d) discharge curves at a current density 2 A g^{-1}; Reprinted with permission. Copyright 2018, American Chemical Society. (e)Schematic illustration for the synthesis of $NiCo_2S_4$ nanoarrays; (f) GCD curves at different current densities of Ni-Co-S/ACC-160; Reprinted with permission. Copyright 2019, Elsevier; (g) The

schematic illustration of the formation process of multi-shell CNHP structure; (h) GCD curves at different current density of TS-CNHP; Reprinted with permission. Copyright 2018, Elsevier. (l) The schematic diagram of the synthesis of M-ZIF-67; (j) GCD curves of M-ZIF-67@LDH in the current density of 0.5-10 A g^{-1}; Reprinted with permission. Copyright 2021, John Wiley and Sons.

Hollow-structured nanomaterials have garnered significant research interest for their promising applications in energy storage due to their high surface area, efficient mass transport, and tunable porosity[153,154]. For instance, Jiang *et al.* synthesized hollow nano-polyhedra using ZIF-67 as a template, systematically investigating the critical roles of shell precipitation and template etching in nanocage formation[155]. The resulting NiCo-LDH nanocages demonstrated excellent pseudocapacitive performance. Bao *et al.* developed a multi-shelled Co/Ni-based hydroxide phosphate (CNHP) hollow polyhedron via a stepwise strategy involving Co/Ni-LDH coating and phosphoric acid etching of ZIF-67 dodecahedra. By precisely controlling LDH deposition and Na_3PO_4 etching duration, they constructed double-shelled (DS-CNHP) and triple-shelled (TS-CNHP) hollow structures shown in Figure 10g. The TS-CNHP exhibited a high specific capacitance of 1,506 F g^{-1} at 1 A g^{-1} and retained 68% of its initial capacitance when the current density increased from 1 to 10 A g^{-1}. A hybrid supercapacitor device assembled with TS-CNHP and activated carbon (AC) achieved a notable energy density of 34.4 Wh kg^{-1} at a power density of 0.375 kW kg^{-1} [Figure 10h]. In related work, our group designed core-shell structures using macro-microporous ZIF-67 (M-ZIF-67) grown on PS templates as the core and LDH as the shell through facile ion etching [Figure 10i]. The optimized material, M-ZIF-67@LDH4, delivered a specific capacitance of 597.6 F g^{-1} at 0.5 A g^{-1} and maintained 92% retention at 3 A g^{-1} [Figure 10j], underscoring the synergistic enhancement from its hierarchical porosity and LDH integration.

The application of etched MOFs in supercapacitors has demonstrated considerable promise. By precisely tailoring the structure and properties of electrode materials, etching strategies have markedly improved key performance metrics including specific

capacitance, rate capability, and cycling stability[156]. Nevertheless, challenges such as limited electrical conductivity, long-term operational stability, and scalable production costs must be addressed to facilitate their practical implementation in commercial supercapacitors[157]. Future research should focus on advancing novel etching methodologies, designing multifunctional composite architectures, and elucidating underlying reaction mechanisms[158]. These efforts are expected to open new avenues for developing high-performance, economically viable supercapacitors.

Battery

Rechargeable batteries including lithium-ion, metal-air, and zinc-manganese systems are extensively utilized across numerous applications due to their high energy density and reversible operation[159]. Etching MOFs has emerged as an efficient strategy for synthesizing advanced electrode materials with superior energy storage performance[160]. The enhancements are primarily attributed to the following structural and functional advantages introduced by etching: (a) Hierarchically porous and hollow structures facilitate rapid ion and electrolyte transport, improving electrode-electrolyte contact; (b) Hollow architectures effectively accommodate volume changes during cycling, enhancing rate capability and long-term cyclability; (c) High specific surface area provides abundant electrochemically active sites, resulting in increased specific capacity.

Etched MOFs have been widely employed as electrodes in various battery systems. Here, we focus on lithium-based batteries, which represent a leading direction in energy storage research. In 2018, Lou's group fabricated multi-shelled nanostructures with tunable shell numbers and evaluated their performance as anodes for lithium-ion batteries[161]. As illustrated in Figure 11a, simply by varying the amount of vanadium oxytriisopropoxide (VOT) during ion exchange with ZIF-67 nanocubes followed by calcination in air, they obtained nanoboxes with single, double, and triple shells. Electrochemical analysis revealed that the triple-shelled nanostructure delivered the most exceptional performance, a result directly attributable to its uniquely engineered architecture[162,163].

The confinement of active nanomaterials within porous carbon matrices has proven to be an effective strategy for enhancing the electrochemical properties of lithium-ion batteries. While carbon materials derived from MOFs hold great promise as electrodes, their inherently small pore sizes often limit accessibility to active sites during cycling[164]. To address this limitation, the same research group developed hollow nanostructures designated as H-Co_3O_4@MCNBs two years later. These consist of hollow Co_3O_4 nanoparticles encapsulated within mesoporous carbon nanoboxes, fabricated through a combination of etching and a carefully controlled two-step thermal treatment that is shown in Figure 11b[165]. This distinctive structure and composition endow the H-Co_3O_4@MCNBs with remarkable lithium storage capabilities as an anode material, including high discharge/charge capacities [Figure 11c] and excellent Coulombic efficiency. In a study by Shin *et al.*, Zn-MOF-5-derived materials were applied in lithium-air batteries to examine the influence of pore characteristics on electrochemical performance[166]. Pore customization was accomplished through controlled heat treatment and etching processes Figure 11d. Unlike the directly carbonized sample C-MOF(1,000), the E-MOF(700-900) series that were fabricated via lower-temperature calcination and ZnO etching exhibited broader pore size distributions and larger mesopores[167]. As depicted in Figure 11e, at a current density of 0.2 mA cm^{-2}, the E-MOF(700-900) electrodes delivered significantly higher discharge capacities than C-MOF(1,000) in lithium-air batteries, owing to the increased accessibility of active sites facilitated by the well-developed mesoporosity[168].

Lithium-sulfur (Li-S) batteries have attracted considerable attention for their high theoretical capacity and energy density. However, practical implementation is hindered by the insulating nature of sulfur, the shuttle effect of polysulfide intermediates, and substantial volume changes during cycling[169]. Hollow frameworks offer a promising solution to accommodate volume expansion and enhance reaction kinetics[170]. Wang and colleagues constructed hollow ZnSe-CoSe heterostructures with tunable cavity sizes through etching of ZIF-8@ZIF-67 precursors followed by gas-phase selenization[171]. As

shown in Figure 11f, varying etching durations produced distinct degrees of hollowing, with the sample labeled 45@ZnSe-CoSe demonstrating the most remarkable electrochemical properties. Furthermore, by integrating 45@ZnSe-CoSe with conductive MXene nanosheets, a high sulfur-loading cathode was achieved. The resulting battery exhibited exceptional performance, highlighting the effectiveness of this hollow heterostructure design in mitigating the challenges of Li-S batteries[172].

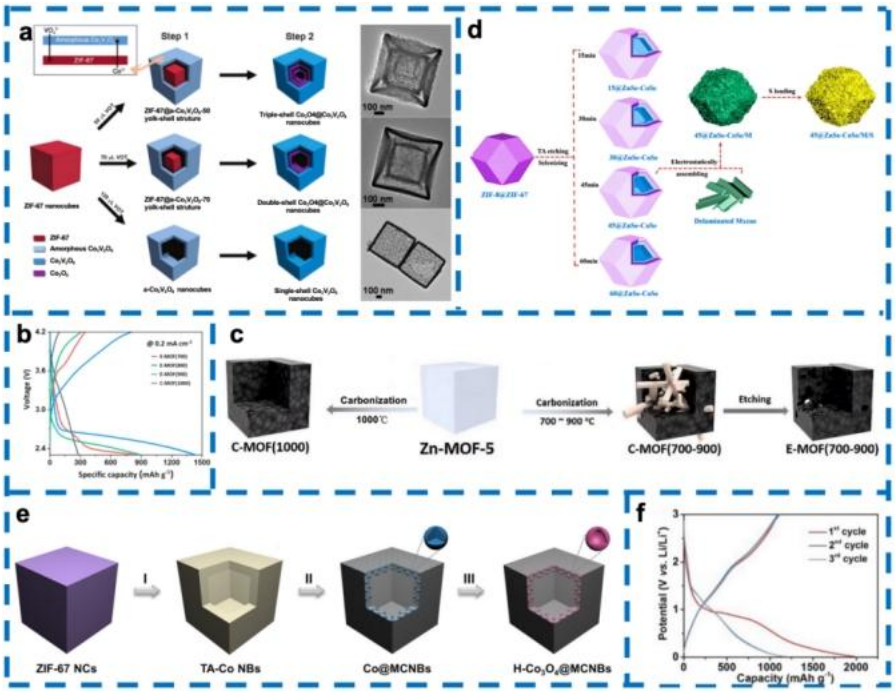

Figure 11. (a) Schematic illustration of the formation of different shelled nanostructures; Reprinted with permission. Copyright 2018, John Wiley and Sons; (b) Initial charge-discharge curves of lithium-air battery at current densities of 0.2 mA cm^{-2}; Reprinted with permission. Copyright 2021, Elsevier; (c)An illustration of the formation process of the 45@ZnSe-CoSe/M/S cathode material; Reprinted with permission. Copyright 2024, Royal Society of Chemistry; (d) Schematic illustration of synthesis of Zn-MOF-5-derived carbon materials; (e) Schematic illustration of the formation process of H-Co_3O_4@MCNBs; (f)galvanostatic discharge-charge voltage profiles for the first three cycles at a current density of 0.2 A g^{-1}; Reprinted with permission. Copyright 2020, John Wiley and Sons.

As evidenced by recent advances, the application of etched MOFs represents a highly promising direction in battery research. Through precise structural and compositional regulation, etching techniques significantly enhance the electrochemical performance of MOF-based electrodes[173]. By selectively removing parts of the framework, etching creates porous or hollow architectures that increase specific surface area and porosity, thereby promoting ion diffusion and improving active site utilization[174].

Moreover, etched MOF structures exhibit improved mechanical stability, effectively mitigating volume changes during ion insertion and extraction. In the context of solid-state batteries, the porous networks formed via etching offer additional ion transport pathways, contributing to higher ionic conductivity of the electrolyte[175,176]. These advantages collectively position etched MOFs and their derivatives as highly competitive materials for next-generation energy storage systems.

Electrochemical sensing

In addition to the above applications, MOFs are also used in electrochemical sensing and demonstrated great potential. By regulating the structures and components, the sensitivity, selectivity and stability of the sensors based on etched MOFs and MOF derivatives have been significantly enhanced[177,178]. Etching facilitates the creation of rich pores to facilitate the diffusion of materials and exposure of plenty surface active sites, enabling the high sensing performance.

In Yao's group, they got the hierarchical hollow MIL-101 cages simply via acid etching and employed in the electrochemical sensor[179]. Attributed to the huge specific surface area and adsorptive property, the hollow MIL-101 denoted high electrocatalytic activity and fantabulous voltammetric response towards the nitrofurazone oxidation. Apparently, compared with solid crystals, the design of hollow structures contributes to extraordinary electrocatalytic activity. Wan and coworkers first developed the *in-situ* growth of ZIF-67 on graphene nanosheets and obtained the sandwich liked nanostructures [Figure 12a][180]. To realize the improvement of electrochemical performance, phytic acid was used to

etch the ZIF-67 polyhedrons to core-shell skeletons. Due to the huge specific surface area and high exposure of active sites, the chemically etched sample PA-ZIF-67@GS illustrated outstanding activity in oxidizing glucose that is shown in Figure 12b. In addition, hollow MOFs with porous structures show promising prospects in the synthesis of high-performance electrochemical luminescence (ECL) materials[181]. Prof. Xiao and colleagues exploited the hydrothermal etching tactics and fabricated the hollow hierarchical UiO-66-NH_2 (HH-UiO-66-NH_2)[182]. Due to the coordinatively unsaturated Zr6 nodes of HH-UiO-66-NH_2 and the hollow pores, $Ru(bpy)_2(mcpbpy)^{2+}$ can be grafted on the skeletons. Surprisingly, HH-Ru-UiO-66-NH_2 demonstrated strong ECL emission [Figure 12c]. What's more, the ECL biosensor tagged by HH-Ru-UiO-66-NH_2 denoted superior detective sensitivity of TB in human serum samples [Figure 12d][183].

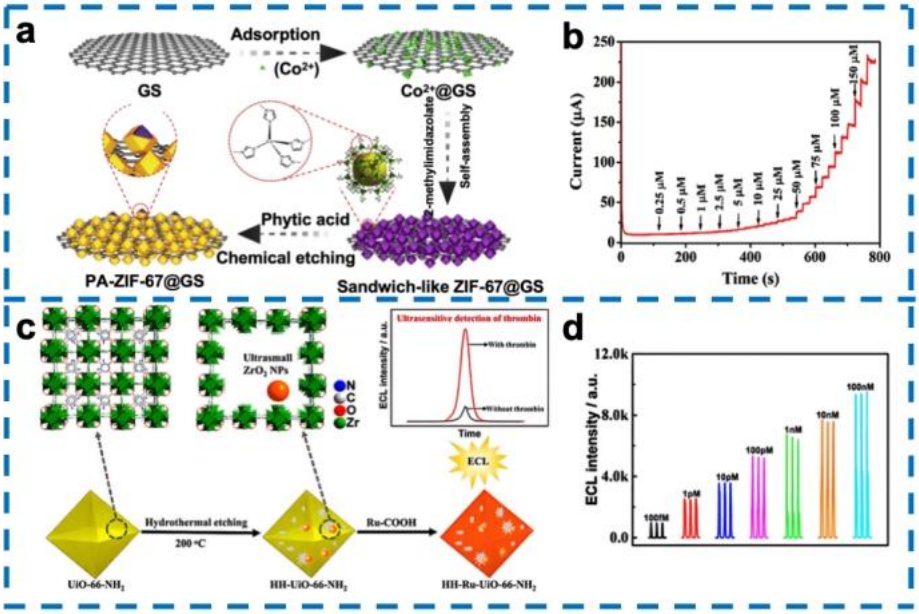

Figure 12. (a) Illustration of the synthesis process of PA-ZIF-67@GS hybrids; (b) *i-t* curves of PA-ZIF-67@GS electrode after the subsequent additions of different concentration of glucose; Reprinted with permission, Copyright 2020, Elsevier; (c) Preparation of HH-Ru-UiO-66-NH_2; (d) ECL responses of different TB concentrations tagged by HH-Ru-UiO-66-NH_2; Reprinted with permission. Copyright 2021, American Chemical Society.

In summary, etching is a useful tool for tailoring the structure, composition, electronics,

and physiochemistry of MOFs, and these beneficial changes help improve the performance of the target application. Future research directions include the development of novel etching techniques, the preparation of multifunctional composite materials, and in-depth studies on the mechanism of reaction, should provide new ideas and methods for the design of high-performance electrochemical sensors.

CONCLUSIONS AND PERSPECTIVE

In this review, we have summarized key strategies for etching MOFs, highlighted the distinctive nanostructures obtained through these processes, and discussed the roles of etched MOFs across various electrochemical applications[184]. Etching significantly enhances mass transport, exposes abundant active sites, and provides void space to accommodate volume changes during energy conversion and storage, collectively improving the overall performance of MOF-based electrodes[185].

It is important to note that etching mechanisms can vary considerably across different MOFs, even when using the same etchant. Therefore, combined experimental and theoretical investigations are essential to elucidate these mechanisms, identify key influencing factors, and optimize etching conditions[186]. For instance, while monocarboxylic acids primarily disrupt UiO-type frameworks through acid-induced coordination cleavage, in ZIFs, proton attack plays a dominant role. Excessive etching must be avoided as it can cause structural collapse and loss of porosity. Parameters such as etchant concentration, temperature, pH, and duration must be carefully controlled to achieve desired pore structures, exposed facets, morphologies, and compositions[187]. Moving forward, the cost efficiency and environmental impact of etching agents and protocols should also be prioritized.

In terms of applications, we have focused on electrocatalytic water splitting, supercapacitors, batteries, and sensors, though the potential of etched MOFs extends well beyond these areas. Long-term stability remains a critical challenge for practical deployment, as etching may compromise mechanical or chemical robustness. Balancing

activity with stability through compositional tuning or integration with stable matrices is often necessary. To harness etched MOFs in high-performance devices, scenario-specific design and precise control over etching processes are imperative.

In summary, etching serves as a powerful tool to tailor the structure, composition, and properties of MOFs for enhanced electrochemical functionality. We hope this review offers a comprehensive overview of the current advances and future directions in etched MOFs, and inspires further innovative research in this rapidly evolving field.

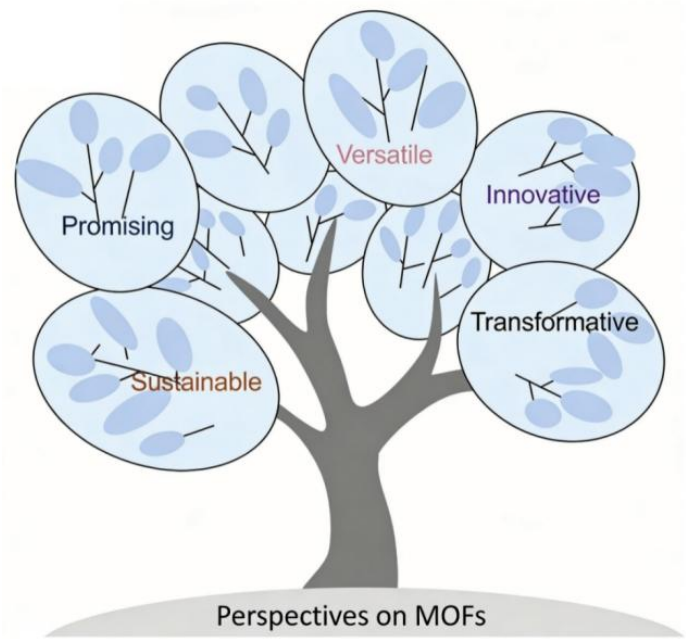

Figure 13. Summary of the future outlook for MOFs.

DECLARATIONS

Authors' contributions

Writing—original draft preparation, data curation, visualization: S.W;

Data curation: J.F;

Visualization, methodology: S.L;

Conceptualization and language polishing: M. S;

Conceptualization, supervision, writing— reviewing and editing, funding acquisition: R.Z;

All authors have read and agreed to the published version of the manuscript.

Availability of data and materials

Data will be made available on request.

Financial support and sponsorship

This work was supported by Natural Science Foundation of Jiangsu Province(BK20230069).

Conflicts of Interest

The authors declare no conflict of interest. Given the role as Editor in Chief, Huan Pang had no involvement in the peer review of this paper and had no access to information regarding its peer-review process. Full responsibility for the editorial process of this paper was delegated to another editor of the journal.

Ethical approval and consent to participate

Not applicable.

Data Availability Statement

Data will be made available on request.

Use of AI and AI-Assisted Technologies

No AI tools were utilized for this paper.

Consent for publication

Not applicable.

Copyright

REFERENCES

1. Chi, J.; Gu, S.; Shi, R.; et al., Extending PANI molecular chains into pores of hierarchical MIL-101 as flexible electrodes for supercapacitor applications. *Chemical Engineering Journal* 2025, 510.[DOI: 10.1016/j.cej.2025.161764]

2. Su, Y.; Shi, Y.; Jin, L.; et al., Unlocking the Potential of MOFs for Waste Plastic Resource Utilization and Microplastic Pollution Control. *Sustainable Engineering Novit* 2026, 2 (1), 4.[DOI: 10.53941/sen.2026.100004]

3. Zhang, X. L.; Tang, Z.; Xu, H. J.; et al., Surface engineering of a MOF-on-MOF heterostructure via selenium oxide embedding for efficient seawater oxygen evolution. *Applied Surface Science* 2026, 727.[DOI: 10.1016/j.apsusc.2026.165837]

4. Zhang, W.; Jiang, X. F.; Zhao, Y. Y.; et al., Hollow carbon nanobubbles: monocrystalline MOF nanobubbles and their pyrolysis. *Chemical Science* 2017, 8 (5), 3538-46.[DOI: 10.1039/C6SC04903F]

5. Feng, J. W.; Liu, L.; Meng, Q. H., Enhanced electrochemical and capacitive deionization performance of metal organic framework/holey graphene composite electrodes. *Journal of Colloid and Interface Science* 2021, 582, 447-58.[DOI: 10.1016/j.jcis.2020.08.091]

6. Fu, R.; Wang, L.; Yang, X.; et al., Defects-Engineered Metal-Organic Frameworks for Supercapacitor Platform. *Sustainable Engineering Novit* 2025, 1 (1), 2.[DOI: 10.53941/sen.2025.100002]

7. Zhang, Y.; Lan, J. H.; Xu, Y. K.; et al., Ultrafine PtCo alloy by pyrolysis etching-confined pyrolysis for enhanced hydrogen evolution. *Journal of Colloid and Interface Science* 2024, 660, 997-1009.[DOI: 10.1016/j.jcis.2024.01.124]

8. Abdi, M. R.; Sarlak, N.; Pourfalah, Z., HKUST-1@etched halloysite nanotube composites for enhanced cryogenic hydrogen adsorption. *Materials Today Communications* 2026, 51.[DOI: 10.1016/j.mtcomm.2026.114647]

9. Acharya, J.; Ojha, G. P.; Kim, B. S.; Pant, B.; Park, M., Modish Designation of Hollow-Tubular rGO-$NiMoO_4$@Ni-Co-S Hybrid Core-shell Electrodes with Multichannel Superconductive Pathways for High-Performance Asymmetric Supercapacitors. *Acs Applied Materials & Interfaces* 2021, 13 (15), 17487-500.[PMID:

33844490 DOI: 10.1021/acsami.1c00137]

10. Aftab, A.; Ahmad, F.; Tunio, S. R.; et al., A critical review on electrochemical behavior of MOF in supercapacitor. *Journal of Organometallic Chemistry* 2025, 1042.[DOI: 10.1016/j.jorganchem.2025.123866]

11. Gao, Y.; Ye, C.; Wang, R.; Li, W.; Pang, H. Hybrid and Flow-Electrode Capacitive Deionization: Materials Design, Multispecies Removal, and Smart Regulation. *Sustainable Engineering Novit* 2025, 1 (1), 7.[DOI: 10.53941/sen.2025.100007]

12. Ahmed, A.; Hodgson, N.; Barrow, M.; et al., Macroporous metal-organic framework microparticles with improved liquid phase separation. *Journal of Materials Chemistry A* 2014, 2 (24), 9085-90.[DOI: 10.1039/C4TA00138A]

13. Yoon, J.; Shin, M.; Lim, J.; Lee, J. Y.; Choi, J. W., Recent Advances in MXene Nanocomposite-Based Biosensors. *Biosensors-Basel* 2020, 10 (11).[PMID: 33233574 PMCID: PMC7699737 DOI: 10.3390/bios10110185]

14. Alekseevskiy, P. V.; Timofeeva, M.; Bachinin, S.; et al., Non-thermal plasma etching of MOF thin films in high optical quality for interference sensing. *Optical Materials* 2024, 154.[DOI: 10.1016/j.optmat.2024.115666]

15. Sun, S.; Zhang, Y.; Wang, M.; et al., Design and Fabrication of Metal-Organic Framework UiO-66 Membranes for Advanced Separation. *Sustainable Engineering Novit* 2026, 2 (1), 3.[DOI: 10.53941/sen.2026.100003]

16. Baby, N.; Thangarasu, S.; Murugan, N.; Kim, Y. A.; Oh, T. H., Emerging SrFe-MOF/Fe-BTC hybrids via post-synthetic induced Fe3+ metal node exchange and nucleation for durable bifunctional electrocatalysis. *Chemical Engineering Journal* 2026, 528.[DOI: 10.1016/j.cej.2025.172235]

17. Ban, Q. F.; Li, L. W.; Liu, H. M.; et al., Polymerization-induced assembly-etching engineering to hollow Co@N-doped carbon microcages for superior electromagnetic wave absorption. *Carbon* 2023, 215.[DOI: 10.1016/j.carbon.2023.118506]

18. Bao, S. X.; Li, J. Y.; Guan, B. Y.; Jia, M. J.; Terasaki, O.; Yu, J. H., A Green Selective Water-Etching Approach to MOF@Mesoporous SiO2 Yolk-Shell Nanoreactors with Enhanced Catalytic Stabilities. *Matter* 2020, 3 (2), 498-508.[DOI: 10.1016/j.matt.2020.06.021]

19. Bindini, E.; Lüdtke, T.; Otaegui, D.; et al., Mind the gap! tailoring sol-gel ceramic mesoporous coatings on labile metal-organic frameworks through kinetic control. *Inorganic Chemistry Frontiers* 2022, 9 (2), 221-30.[DOI: 10.1039/D1QI01128F]

20. Liang, Z.; Xie, J.; Liu, Q.; et al., Recent Progress of Metal-Organic Frameworks and Derivatives for High-Performance Aqueous Zinc-Based Batteries. *Sustainable Engineering Novit* 2026, 2 (1), 2.[DOI: 10.53941/sen.2026.100002]

21. Dong, J. N.; Zhang, X. N.; Dong, X. L.; et al., Coupled porosity and heterojunction engineering: MOF-derived porous Co_3O_4 embedded on TiO_2 nanotube arrays for water remediation. *Chemosphere* 2021, 274.[DOI: 10.1016/j.chemosphere.2021.129799]

22. Chen, X. C.; Liu, H.; Wang, L.; Wang, B., Morphology Engineering of Metal-Organic Frameworks by Facet-Selective Protection and Etching. *Inorganic Chemistry* 2024, 63 (34), 15574-8.[DOI: 10.1021/acs.inorgchem.4c02837]

23. Chen, H.; Gu, Z. G.; Mirza, S.; Zhang, S. H.; Zhang, J., Hollow Cu-TiO2/C nanospheres derived from a Ti precursor encapsulated MOF coating for efficient photocatalytic hydrogen evolution. *Journal of Materials Chemistry A* 2018, 6 (16), 7175-81.[DOI: 10.1039/C8TA01034J]

24. Li, S. S.; Gao, Y. Q.; Li, N.; Ge, L.; Bu, X. H.; Feng, P. Y., Transition metal-based bimetallic MOFs and MOF-derived catalysts for electrochemical oxygen evolution reaction. *Energy & Environmental Science* 2021, 14 (4), 1897-927.[DOI: 10.1039/D0EE03697H]

25. Lv, S. W.; Zhao, N.; Liu, J. M.; Yang, F. E.; Li, C. Y.; Wang, S., Newly Constructed NiCo2O4 Derived from ZIF-67 with Dual Mimic Enzyme Properties for Colorimetric Detection of Biomolecules and Metal Ions. *Acs Applied Materials & Interfaces* 2021, 13 (21), 25044-52.[PMID: 34019375 DOI: 10.1021/acsami.1c06705]

26. Tang, Z.; Wei, A., Fabrication of Anisotropic Metal Nanostructures Using Innovations in Template-Assisted Lithography. *Acs Nano* 2012, 6 (2), 998-1003.[PMID: 22324475 PMCID: PMC3302161 DOI: 10.1021/nn300375r]

27. Drozhzhin, N. A.; Ponomareva, O. Y.; Vinogradov, II; et al., Nickel (II) Based Metal-Organic Framework Consolidated on Nanofibers Modified Track-Etched Membrane for Dye Removal. *Eurasian Journal of Chemistry* 2025, 119 (3),

118-28.[DOI: 10.31489/2959-0663/3-25-7]

28. Chhetri, K.; Dahal, B.; Tiwari, A. P.; et al., Controlled Selenium Infiltration of Cobalt Phosphide Nanostructure Arrays from a Two-Dimensional Cobalt Metal-Organic Framework: A Self-Supported Electrode for Flexible Quasi-Solid-State Asymmetric Supercapacitors. *Acs Applied Energy Materials* 2021, 4 (1), 404-15.[DOI: 10.1021/acsaem.0c02340]

29. Chen, L. L.; Liu, Y. X.; Su, Y. C.; Zhu, W. C.; Du, G. Y.; Pang, H., Research progress in metal-organic frameworks and their derivatives in electrochemistry. *Science China-Chemistry* 2025, 68 (4), 1287-316.[DOI: 10.1007/s11426-024-2277-2]

30. He, Y. Y.; Fang, J.; Zhang, W. Y.; et al., High-efficiency oxygen evolution electrocatalysis enabled by Ar/O2 plasma-induced synergistic modifications in NiFe Prussian blue analogue systems. *Rsc Advances* 2025, 15 (43), 36206-12.[DOI: 10.1039/D5RA03979G]

31. Qu, N.; Xu, G. X.; et al., Multi-Scale Design of Metal-Organic Framework Metamaterials for Broad-Band Microwave Absorption. *Advanced Functional Materials* 2025, 35 (18).[DOI: 10.1002/adfm.202402923]

32. Garg, R.; Alattar, B.; Sabouni, R.; Ghommem, M., "Turn-on" fluorescence-based diclofenac detection using metal-organic framework-coated silicon micropillars. *Journal of Water Process Engineering* 2025, 76.[DOI: 10.1016/j.jwpe.2025.108240]

33. Goswami, A.; Ghosh, D.; Pradhan, D.; Biradha, K., In Situ Grown Mn(II) MOF upon Nickel Foam Acts as a Robust Self-Supporting Bifunctional Electrode for Overall Water Splitting: A Bimetallic Synergistic Collaboration Strategy. *Acs Applied Materials & Interfaces* 2022, 14 (26), 29722-34.[DOI: 10.1021/acsami.2c04304]

34. Gourji, F. H.; Rajaramanan, T.; Kishore, A.; Heggertveit, M.; Velauthapillai, D., Hierarchical Cube-in-Cube Cobalt-Molybdenum Phosphide Hollow Nanoboxes Derived from the MOF Template Strategy for High-Performance Supercapacitors. *Acs Omega* 2023, 8 (26), 23446-56.[DOI: 10.1021/acsomega.3c00337]

35. Gu, X. C.; Ji, Y. G.; Tian, J. Q.; Wu, X.; Feng, L. G., Combined MOF derivation and fluorination imparted efficient synergism of Fe-Co fluoride for oxygen evolution reaction. *Chemical Engineering Journal* 2022, 427.[DOI: 10.1016/j.cej.2021.131576]

36. Gu, Z. Y.; Yang, C. X.; Chang, N.; Yan, X. P., Metal-Organic Frameworks for Analytical Chemistry: From Sample Collection to Chromatographic Separation. *Accounts of Chemical Research* 2012, 45 (5), 734-45.[DOI: 10.1021/ar2002599]

37. Sahoo, S.; Rout, C. S., Facile Electrochemical Synthesis of Porous Manganese-Cobalt-Sulfide Based Ternary Transition Metal Sulfide Nanosheets Architectures for High Performance Energy Storage Applications. *Electrochimica Acta* 2016, 220, 57-66.[DOI: 10.1016/j.electacta.2016.10.043]

38. Hong, L. X.; Yang, Q. Q.; Zhang, R. L.; Zhao, J. S., A Novel Strategy Synthesized Highly Specific Surface Area Bimetallic CoMn-MOFs as Electrode Materials for Supercapacitors. *Journal of Inorganic and Organometallic Polymers and Materials* 2025, 35 (10), 8391-403.[DOI:10.1007/s10904-025-03802-8]

39. Hu, Y. X.; Wu, Y. Q.; Devendran, C.; et al., Preparation of nanoporous graphene oxide by nanocrystal-masked etching: toward a nacre-mimetic metal-organic framework molecular sieving membrane. *Journal of Materials Chemistry A* 2017, 5 (31), 16255-62.[DOI: 10.1039/C7TA00927E]

40. Huang, H. L.; Sun, Y. X.; Jia, X. M.; et al., Air-Steam Etched Construction of Hierarchically Porous Metal-Organic Frameworks. *Chinese Journal of Chemistry* 2021, 39 (6), 1538-44.[DOI: 10.1002/cjoc.202000718]

41. Wang, D. X.; Zhu, F.; Dang, Y. P.; et al., Conformal phosphating hierarchical interface of CC/CoNiMn-P for hybrid supercapacitors with high cycling stability. *Inorganic Chemistry Frontiers* 2025, 12 (8), 3098-109.[DOI: 10.1039/D5QI00123D]

42. Chen, F. J.; Mu, X. Q.; Zhou, J. L.; et al., Engineering the Active Sites of MOF-derived Catalysts: From Oxygen Activation to Activate Metal-Air Batteries. *Chinese Journal of Chemistry* 2024, 42 (20), 2520-35.[DOI: 10.1002/cjoc.202400332]

43. Chen, L.; Cheng, H.; Hu, R.; et al., Kirkendall Effect-Mediated Transformation of ZIF-67 to NiCo-LDH Nanocages as Oxidase Mimics for Multicolor Point-of-Care Testing of β-Galactosidase Activity and Escherichia coli. *Analytical Chemistry* 2025, 97 (5), 2853-62.[DOI: 10.1021/acs.analchem.4c05379]

44. Chen, Z. B.; Wang, J. K.; Lu, L.; et al., Corrosion-oriented self-healing coating based on ZnMg MOF for efficient corrosion protection of aluminum alloy via in-situ LDH film

formation. *Chemical Engineering Journal* 2024, 500.[DOI: 10.1016/j.cej.2024.156898]

45. Yin, H. R.; Liu, X. Q.; Wang, L. X.; Isimjan, T. T.; Cai, D. D.; Yang, X. L., Real Active Site Identification of Co/Co_3O_4 Anchoring Ni-MOF Nanosheets with Fast OER Kinetics for Overall Water Splitting. *Inorganic Chemistry* 2024, 63 (15), 7045-52.[PMID: 38569164 DOI: 10.1021/acs.inorgchem.4c00712]

46. Chen, Z. C.; Fu, X. Y.; Jiang, H.; et al., Cationic hybridization produces core-shell structure MOF derivatives for reducing electromagnetic pollution. *Chemical Engineering Science* 2023, 280.[DOI: 10.1016/j.ces.2023.118966]

47. Cheng, D.; Li, P. P.; Xu, Z. J.; et al., Signal On-Off Electrochemical Sensor for Glutathione Based on a AuCu-Decorated Zr-Containing Metal-Organic Framework via Solid-State Electrochemistry of Cuprous Chloride. *Acs Sensors* 2022, 7 (8), 2465-74.[DOI: 10.1021/acssensors.2c01221]

48. Wang, P.; Yang, C.; Yao, J. S.; et al., Two-dimensional metal organic framework nanosheets in electrocatalysis. *Chemical Science* 2025, 16 (16), 6583-97.[PMCID: PMC11955774 PMID: 40171025]

49. Wei, W. H.; Luo, S. J.; Zhao, Y.; et al., A solution-assisted etching preparation of an MOF-derived NH4CoPO4•H2O/Ti3C2Tx MXene nanocomposite for high-performance hybrid supercapacitors. *New Journal of Chemistry* 2021, 45 (25), 11174-82.[DOI: 10.1039/D1NJ01394G]

50. Murugasamy, J.; Ramasundaram, S.; Mishra, N. K.; et al., Development of alkali-etched ZIF-67 metal-organic framework composite incorporated PVDF UF membranes for efficient wastewater treatment. *Journal of the Taiwan Institute of Chemical Engineers* 2026, 179.[DOI: 10.1016/j.jtice.2025.106424]

51. Zhai, H. C.; Zhang, G. J.; Zhang, Z. W.; et al., Ultrahigh gas response of chlorine sensor based on In2O3 multibeam pores by etching precursor MOFs with urea. *Journal of Environmental Chemical Engineering* 2025, 13 (5).[DOI: 10.1016/j.jece.2025.118027]

52. Lee, S. J.; Lee, G. H. Y.; Oh, M., MOF-on-MOF Growth: Inducing Naturally Nonpreferred MOFs and Atypical MOF Growth. *Accounts of Chemical Research* 2024, 57 (21), 3113-25.[PMID: 39388366 DOI: 10.1021/acs.accounts.4c00469]

53. Song, X.; Zou, Y.; Liu, X.; Oh, M.; Lah, M. S., A two-fold interpenetrated (3,6)-connected metal-organic framework with rutile topology showing a large solvent cavity. *New Journal of Chemistry* 2010, 34 (11), 2396-9.[DOI: 10.1039/C0NJ00272K]

54. Deng, L. P.; Liu, P.; Xiao, H. Y.; et al., In-situ architecting hydrophilic, defect-rich MgMn-MOF on bimetallic oxide loaded biochar for smartphone-operated portable electrochemical-colorimetric dual-mode intelligent sensing of Cu2+in rice plants. *Sensors and Actuators B-Chemical* 2025, 439.[DOI: 10.1016/j.snb.2025.137859]

55. Ding, J. Y.; Sun, Q.; Zhong, L.; et al., Thermal conversion of hollow nickel-organic framework into bimetallic FeNi3 alloy embedded in carbon materials as efficient oer electrocatalyst. *Electrochimica Acta* 2020, 354.[DOI: 10.1016/j.electacta.2020.136716]

56. Pravin, M. B. S.; Mazhar, W.; Alshamari, A.; et al., MOF-Assisted Synthesis of Hierarchically Porous ZIF-67-Derived Co_3O_4 Nanosheets Enabling High Specific Capacitance and Long-Cycle Stability for High-Current-Density Supercapacitors. *Journal of Electronic Materials* 2026.[DOI: 10.1007/s11664-026-12744-x]

57. Wang, Q. B.; Luo, J. H.; Wu, Y. H.; Xie, Y.; Cheng, L. C., Tunable Electromagnetic Response Behaviors via Cross-Scale Morphological Structural Engineering for Ultra-wideband Microwave Absorption. *Chinese Journal of Chemistry* 2025, 43 (21), 2756-70.[DOI: 10.1002/cjoc.70169]

58. Li, H. N.; Li, Y. F.; Liu, Y. Z.; Guo, J. C.; Yi, Z. L., Hierarchical collaborative architecture of MOF-derived cobalt phosphide-porous carbon conductive networks: enabling high-performance supercapacitor energy storage. *Applied Surface Science* 2026, 730.[DOI: 10.1016/j.apsusc.2026.166369]

59. Lei, J. L.; Li, S. S.; Zhen, X.; Shen, L.; He, B., Pr-doped NiFe-layered double hydroxide on plasma-etched nickel foam as a high-efficiency electrocatalyst for oxygen evolution reaction. *Dalton Transactions* 2026, 55 (5), 2071-9.[DOI: 10.1039/D5DT02658J]

60. Chen, M. T.; Jiang, Z. G.; Wang, R. Z.; et al., Polymetallic Prussian blue analogues with hierarchical structure for high efficiency oxygen evolution reactions. *International Journal of Hydrogen Energy* 2024, 54, 963-70.[DOI: 10.1016/j.ijhydene.2023.11.181]

61. Li, S. S.; Wu, P. J.; Ming, Z. Y.; Liu, C. H.; Wang, W. C.; Chen, Z. D., A De Novo

Sacrificial-MOF Strategy for Fabricating Cellulose Nanofibers/ZIF-8/PANI Gel Composite Membranes for High-Performance Flexible Supercapacitors. *Gels* 2026, 12 (2).[DOI: 10.3390/gels12020134]

62. Yadnum, S.; Roche, J.; Lebraud, E.; et al., Site- Selective Synthesis of Janus- type Metal-Organic Framework Composites. *Angewandte Chemie-International Edition* 2014, 53 (15), 4001-5.[PMID: 24604879 DOI: 10.1002/anie.201400581]

63. Li, H.; Shu, C. G.; Chen, G.; et al., Dual-templates-assisted synthesis of hollow nanoreactors with hierarchically porous shell for efficient oxygen reduction reaction. *Fuel* 2025, 402.[DOI: 10.1016/j.fuel.2025.136058]

64. Herrera-Herrera, P. A.; Rodríguez-Sevilla, E.; Varela, A. S., The role of the metal center on charge transport rate in MOF-525: cobalt and nickel porphyrin. *Dalton Transactions* 2021, 50 (46), 16939-44.[DOI: 10.1039/D1DT03435A]

65. Apostol, P.; Gali, S. M.; Su, A.; et al., Controlling Charge Transport in 2D Conductive MOFs-The Role of Nitrogen-Rich Ligands and Chemical Functionality. *Journal of the American Chemical Society* 2023, 145 (45), 24669-77.[DOI: 10.1021/jacs.3c07503]

66. Chen, X.; Zhang, K.; Hassan, Z. M.; Redel, E.; Baumgart, H., Charge. transport, conductivity and Seebeck coefficient in pristine and TCNQ loaded preferentially grown metal-organic framework films. *Journal of Physics-Condensed Matter* 2022, 34 (40).[PMID: 33596560 DOI: 10.1088/1361-648X/abe72f]

67. Hu, H.; Xie, H. H.; Liang, S. Q.; et al., Fabricating MOF-Supported Nonprecious Metal Nanocatalysts from the Commercial Metal Dusts via a Mechanochemistry-Assisted Sacrificial Strategy. *Inorganic Chemistry* 2025, 64 (43), 21674-82.[PMID: 41108267 DOI: 10.1021/acs.inorgchem.5c03892]

68. Hu, P. Y.; Qin, H. C.; et al., Constructing a defect-rich hydroxide nanoenzyme sensor based on dielectric barrier discharge microplasma etching for sensitive detection of thiamine hydrochloride and hydrogen peroxide. *Journal of Colloid and Interface Science* 2022, 628, 597-606.[PMID: 35940144 DOI: 10.1016/j.jcis.2022.07.151]

69. Qin, H. C.; Dai, R.; Hu, P. Y.; et al., Constructing a hollow-cage nanoenzyme sensor for dual detection of thiamine hydrochloride and hydrogen peroxide based on dielectric

barrier discharge microplasma etching. *Microchemical Journal* 2024, 207.[PMID: 35940144 DOI: 10.1016/j.jcis.2022.07.151]

70. Yu, S. W.; Li, C.; Zhao, S. K.; et al., Recent advances in the interfacial engineering of MOF-based mixed matrix membranes for gas separation. *Nanoscale* 2024, 16 (16), 7716-33.[PMID: 38536054 DOI: 10.1039/d4nr00096j]

71. Zhang, S. T.; Wang, C. G.; Meng, X. W.; et al., Enhanced electromagnetic wave absorption of multicore Fe4N@N-doped porous carbon core-shell microspheres through dielectric-magnetic coordination. *Carbon* 2025, 237.[DOI: 10.1016/j.carbon.2025.120176]

72. Liu, L.; Xia, Z. Q.; Li, S. B.; Zhang, Y. J.; Wang, N., MOF-derived double-shelled Fe(OH)3@NiCo-LDH hollow cubes and their efficient adsorption for anionic organic pollutant. *Journal of Porous Materials* 2022, 29 (3), 931-45.[DOI: 10.1007/s10934-022-01220-6]

73. Li, H.; Lin, H. J.; Raza, S.; et al., Construction of MXene-MOF membranes with photocatalytic self-cleaning for enhanced oil-water emulsion separation. *Journal of Membrane Science* 2025, 718.[DOI: 10.1016/j.memsci.2024.123685]

74. Qiu, M.; Wang, Y.; Liu, Y. N.; Shen, Z. F., Defect Remediation of MXene Membranes Facilitated by Intercalation and Coordination Processes for Enhanced Organic Pollutant Removal. *Acs Applied Nano Materials* 2025, 8 (37), 18070-9.[DOI: 10.1021/acsanm.5c03186]

75. Park, S.; Ryu, J.; Cho, H. Y.; Sohn, D., Halloysite nanotubes loaded with HKUST-1 for CO2 adsorption. *Colloids and Surfaces a-Physicochemical and Engineering Aspects* 2022, 651.[DOI: 10.1016/j.colsurfa.2022.129750]

76. Zhang, C.; Liao, P. Y.; Wang, H.; Sun, J.; Gao, P., Preparation of novel bimetallic CuZn-BTC coordination polymer nanorod for methanol synthesis from CO2 hydrogenation. *Materials Chemistry and Physics* 2018, 215, 211-20.[DOI: 10.1016/j.matchemphys.2018.05.028]

77. Zeng, H. C.; Qiu, P. F.; Huang, Z.; Tan, X. N.; Huang, Z. Y.; Zhou, Y., Controllable synthesis and morphology engineering of S-doped NiCo layered double hydroxide nanoflowers for high-performance supercapacitors. *Journal of Power Sources* 2026,

665.[DOI: 10.1016/j.jpowsour.2025.238966]

78. Ulisso, D. M.; Mane, S. A.; Chavan, R. A.; Kamble, G. P.; Kolekar, S. S.; Ghule, A. V., Multilayered core-shell NiCo-layered double hydroxide@NiCo2O4 composite electrode for high-performance supercapacitor. *Journal of Alloys and Compounds* 2024, 980.[DOI: 10.1016/j.jallcom.2024.173563]

79. Main, R. M.; Cordes, D. B.; Desai, A. V.; et al., Solvothermal Synthesis of a Novel Calcium Metal-Organic Framework: High Temperature and Electrochemical Behaviour. *Molecules* 2021, 26 (22).[PMID: 34834138 PMCID: PMC8623775 DOI: 10.3390/molecules26227048]

80. Deyko, G. S.; Kravtsov, L. A.; Glukhov, L. M.; et al., ynthesis and adsorption properties of new calcium metal-organic framework (Ca-MOF) ZIOC-10 based on a new carbazole linker. *Microporous and Mesoporous Materials* 2024, 373.[DOI: 10.1016/j.micromeso.2024.113120]

81. Zheng, Y. H.; Hu, H. T.; Zhu, Y.; et al., ZIF-67-Derived (NiCo)S2@NC Nanosheet Arrays Hybrid for Efficient Overall Water Splitting. *Inorganic Chemistry* 2022, 61 (36), 14436-46.[PMID: 36038523 DOI: 10.1021/acs.inorgchem.2c02375]

82. Pan, Y.; Sun, K. A.; Liu, S. J.; et al., Core-Shell ZIF-8@ZIF-67-Derived CoP Nanoparticle-Embedded N-Doped Carbon Nanotube Hollow Polyhedron for Efficient Overall Water Splitting. *Journal of the American Chemical Society* 2018, 140 (7), 2610-8.[PMID: 29341596 DOI: 10.1021/jacs.7b12420]

83. Liu, Z. X.; He, K.; Yang, Z. G.; et al., Plasma-Induced Reconstruction of CoNi-MOF-74 into Nanoporous Surfaces at Room Temperature for Enhanced Oxygen Evolution Reaction. *Acs Applied Nano Materials* 2025, 8 (48), 23016-26.[DOI: 10.1021/acsanm.5c04043]

84. Yi, F. Y.; Zhang, R.; Wang, H. L.; et al., Metal-Organic Frameworks and Their Composites: Synthesis and Electrochemical Applications. *Small Methods* 2017, 1 (11).[DOI: 10.1002/smtd.201700187]

85. Guan, B. Y.; Yu, X. Y.; Wu, H. B.; Lou, X. W., Complex Nanostructures from Materials based on Metal-Organic Frameworks for Electrochemical Energy Storage and Conversion. *Advanced Materials* 2017, 29 (47).[PMID: 28960488 DOI:

10.1002/adma.201703614]

86. Lan, Y. Z.; Yu, R.; Wang, Q.; Dai, J. F., Synthesis of ultra-high specific surface area trimetallic NiCoMg-LDH hollow cage via bimetallic ion etching for hybrid supercapacitors. *Ionics* 2024, 30 (5), 3033-44.[DOI: 10.1007/s11581-024-05493-6]

87. Gao, Y. F.; Zhao, Z. H.; Ma, M. H.; et al., Eu-MOF@Ce-MOF heterostructure and molecularly imprinted polymer composite system for SARS-CoV-2 point-of-care detection. *Talanta* 2026, 303.[PMID: 41619327 DOI: 10.1016/j.talanta.2026.129477]

88. Li, H. J.; Sun, Y. C.; Guan, J. Y.; et al., Amidoxime-functionalized PIM-1 incorporating defect-engineered ZIF-8 for enhanced propylene/propane separation and plasticization resistance. *Journal of Membrane Science* 2025, 722.[DOI: 10.1016/j.memsci.2025.123907]

89. Yu, Z. J.; Sun, Y. X.; Zhang, Z. Q.; Geng, C. X.; Qiao, Z. H., Rational Matching of Metal-Organic Frameworks and Polymers in Mixed Matrix Membranes for Efficient Propylene/Propane Separation. *Polymers* 2024, 16 (17).[PMID: 39274177 PMCID: PMC11398130 DOI: 10.3390/polym16172545]

90. Xia, W.; Tang, J.; Li, J. J.; et al., Defect-Rich Graphene Nanomesh Produced by Thermal Exfoliation of Metal-Organic Frameworks for the Oxygen Reduction Reaction. *Angewandte Chemie-International Edition* 2019, 58 (38), 13354-9.[PMID: 31407475 DOI: 10.1002/anie.201906870]

91. Liu, Y. Z.; Hu, J. W.; Zhu, Q. Y.; et al., Preparation of NiCo-LDH composite materials derived from NiCo-MOF by alkaline etching for high performance supercapacitor. *Journal of Physics and Chemistry of Solids* 2025, 206.[DOI: 10.1016/j.jpcs.2025.112834]

92. Wang, X. L.; Wang, M.; Chen, M. L.; Zhang, Y. T., A Mini Review of Ceramic-Based MOF Membranes for Water Treatment. *Membranes* 2023, 13 (9).[PMID: 37755173 PMCID: PMC10537879 DOI: 10.3390/membranes13090751]

93. Wang, Y. R.; Yang, G. Z.; Chao, M.; et al., Molten Salts Etching Driven In-Situ Construction of MOF-Derived Co/Co-N-C/MXene toward Oxygen Reduction Catalysis. *Energy & Fuels* 2025, 39 (17), 8283-90.[DOI: 10.1021/acs.energyfuels.5c00357]

94. Li, J. W.; Xu, J. L.; Zhao, J.; et al., Modulation of oxygen-etching for generating

nickel single atoms for efficient electroreduction of CO2 to syngas (CO/H2). *Journal of Catalysis* 2023, 421, 332-341.[DOI: 10.1016/j.jcat.2023.03.029]

95. Absalan, Y.; Mokari, F.; Delaram, B.; Gholizadeh, M.; Suri, K., Optoelectronic Alteration of Metal-Organic Frameworks for Enhanced Photocatalytic Water Splitting Activity Under Solar Radiation. *Comments on Inorganic Chemistry* 2024, 44 (4), 235-312.[DOI: 10.1080/02603594.2023.2285064]

96. Liu, Z. Y.; An, T.; Luo, Y. H.; Wang, X.; Su, H.; Zhang, D. E., Dual engineering of pores and surfaces in metal-organic frameworks via precision etching for enhanced photocatalytic performance. *Journal of Materials Chemistry A* 2025, 13 (23), 17541-52.[DOI: 10.1039/D5TA01490E]

97. Sun, W.; Zhang, X.; Zhu, H. Q.; et al.,Hollow metal-organic frameworks micro-/nanoreactors via in-situ cascade engineering: boosting neurotransmitter sensitive recognition. *Advanced Composites and Hybrid Materials* 2025, 9 (1).[DOI: 10.1007/s42114-025-01574-w]

98. Lin, Z. Q.; Guo, M. L.; Wang, Y. F.; et al., Accelerated structural transformation of metal-organic frameworks via interfacial engineering for efficient oxygen evolution reaction. *International Journal of Hydrogen Energy* 2024, 85, 766-72.[DOI: 10.1016/j.ijhydene.2024.08.401]

99. Wang, W. J.; Chen, D.; Li, F. Y.; Xiao, X.; Xu, Q., Metal-organic-framework-based materials as platforms for energy applications. *Chem* 2024, 10 (1), 86-133.[DOI: 10.1016/j.chempr.2023.09.009]

100. Sumida, K.; Liang, K.; Reboul, J.; Ibarra, I. A.; Furukawa, S.; Falcaro, P., Sol-Gel Processing of Metal-Organic Frameworks. *Chemistry of Materials* 2017, 29 (7), 2626-45.[DOI: 10.1021/acs.chemmater.6b03934]

101. Zhao, W. B.; Zeng, Y. T.; Zhao, Y. H.; Wu, X. L., Recent advances in metal-organic framework-based electrode materials for supercapacitors: A review. *Journal of Energy Storage* 2023, 62.[DOI: 10.1016/j.est.2023.106934]

102. Wei, T.; Lu, J. H.; Wang, M. T.; et al., MOF-Derived Materials Enabled Lithiophilic 3D Hosts for Lithium Metal Anode - A Review. *Chinese Journal of Chemistry* 2023, 41 (15), 1861-74.[DOI: 10.1002/cjoc.202200816]

103. Liu, F. F.; Zuo, P.; Li, J.; et al., A layered multifunctional framework based on polyacrylonitrile and MOF derivatives for stable lithium metal anode. *Journal of Energy Chemistry* 2024, 93, 282-8.[DOI: 10.1016/j.jechem.2024.02.014]

104. Ren, Y. M.; Xu, Y. X., Three-dimensional graphene/metal-organic framework composites for electrochemical energy storage and conversion. *Chemical Communications* 2023, 59 (43), 6475-94.[DOI: 10.1039/D3CC01167D]

105. Li, X. X.; Feng, X. Y.; Meng, D. L.; et al., Fabrication of TiO2/MOF Type II Heterojunction by Growth of TiO2 on Cr-Based MOF for Enhanced Photocatalytic Hydrogen Production. *Crystal Growth & Design* 2025, 25 (4), 1182-9.[DOI: 10.1021/acs.cgd.4c01530]

106. Ren, S. B.; Jin, Y. X.; Wang, R. Q.; Wang, T. H.; Chen, P., In-situ growth of Li4Ti5O12 on MXene and self-assembly with hollow Co/C microspheres to form an ultra-broadband and high-performance microwave absorber. *Chemical Engineering Journal* 2025, 522.[DOI: 10.1016/j.cej.2025.167835]

107. Lee, Y.; Bae, S.; Kim, J. W.; et al., Metal surface passivation in semiconductor processing of Mo, W, TiN/ TiSiN, and Cu: emerging strategies for corrosion and etching control. *Materials & Design* 2026, 263.[DOI:10.1016/j.matdes.2026.115650]

108. Murugesan, A.; Li, H. H.; Shoaib, M., Recent Advances in Functionalized Carbon Quantum Dots Integrated with Metal-Organic Frameworks: Emerging Platforms for Sensing and Food Safety Applications. *Foods* 2025, 14 (12).[DOI: 10.3390/foods14122060]

109. Wang, Y. J.; Zhang, P.; Hou, C. T., Imparting functionality into porphyrin metal-organic framework aerogels with uniform distributions for diversified applications. *Microporous and Mesoporous Materials* 2025, 381.[DOI: 10.1016/j.micromeso.2024.113355]

110. Li, Y. B.; Chen, H. D.; Zhang, H.; et al., In Situ Etching Strategy to Controllably Fabricate Single-Crystal Metal-Organic Framework Microtubes. *Crystal Growth & Design* 2022, 22 (3).[DOI: 10.1021/acs.cgd.1c01234]

111. Song, J. Y.; Yu, Y. Y.; Han, X. S.; et al., Novel MOF(Zr)-on-MOF(Ce) adsorbent for elimination of excess fluoride from aqueous solution. *Journal of Hazardous Materials*

2024, 463.[DOI: 10.1016/j.jhazmat.2023.132843]

112. Xu, H. D.; Han, J.; Zhao, B.; et al., A facile dual-template-directed successive assembly approach to hollow multi-shell mesoporous metal-organic framework particles. *Nature Communications* 2023, 14 (1).[PMID: 38052827 PMCID: PMC10698178 DOI: 10.1038/s41467-023-43259-2]

113. Shen, X. D.; Huang, L. P.; Li, S. S.; et al., Trimetallic MOF-derived CoFeNi/Z-P NC nanocomposites as efficient catalysts for oxygen evolution reaction. *Dalton Transactions* 2023, 52 (47), 17711-6.[PMID: 37902882 DOI: 10.1039/d3dt02818f]

114. Narciso, J.; Ramos-Fernandez, E.; Delgado-Marín, J. J.; Affolter, C. W.; Olsbye, U.; Redekop, E. A., New route for the synthesis of Co-MOF from metal substrates. *Microporous and Mesoporous Materials* 2021, 324.[DOI; 10.1016/j.micromeso.2021.111310]

115. Mai, J. H.; Zhang, Y. L.; He, H.; et al., Metal-support interface engineering for stable and enhanced hydrogen evolution reaction. *Materials Today Chemistry* 2024, 38.[DOI:10.1016/j.mtchem.2024.102079]

116. Chai, L. L.; Pan, J. Q.; Hu, Y.; Qian, J. J.; Hong, M. C., Rational Design and Growth of MOF-on-MOF Heterostructures. *Small* 2021, 17 (36).[PMID: 34245231 DOI: 10.1002/smll.202100607]

117. Jiang, Y. F.; Zhang, Z. Y.; Du, Y. J.; Jiao, J. W.; Bian, Y.; Cai, D.; Shan, H. C., Tailoring the architecture of metal-organic frameworks: Precision etching for engineered defects and surfaces. *Green Energy & Environment* 2025, 10 (11).[DOI: 10.1016/j.gee.2025.09.006]

118. Luo, J. B.; Wang, X. Z.; Wang, S. T.; et al., MOF-derived S-doped NiCo2O4 hollow cubic nanocage for highly efficient electrocatalytic oxygen evolution. *Journal of Colloid and Interface Science* 2024, 656, 297-308.[PMID: 37995400 DOI: 10.1016/j.jcis.2023.11.094]

119. Yang, H.; Kruger, P. E.; Telfer, S. G., Metal-Organic Framework Nanocrystals as Sacrificial Templates for Hollow and Exceptionally Porous Titania and Composite Materials. *Inorganic Chemistry* 2015, 54 (19), 9483-90.[PMID: 26365676 DOI: 10.1021/acs.inorgchem.5b01352]

120. Ipadeola, A. K.; Eid, K.; Abdullah, A. M.; Ozoemena, K. I., Pd-Nanoparticles Embedded Metal-Organic Framework-Derived Hierarchical Porous Carbon Nanosheets as Efficient Electrocatalysts for Carbon Monoxide Oxidation in Different Electrolytes. *Langmuir* 2022.[PMID: 36040806 DOI: 10.1021/acs.langmuir.2c01841]

121. Cao, K.; Yuan, G.; Liu, M.; Lu, S.; Shin, B.-C.; Yu, L. Organoselenium Catalyzed Reaction: Sustainable Chemistry from Laboratory to Industry. *Sustainable Engineering Novit* 2025, 1 (1), 1.[DOI: 10.53941/sen.2025.100001]

122. Yan, W.; Liao, M. C.; Luo, C. W.; Zhang, K.; Wu, G. Z.; Zeng, H. Y., CoAl2O4 quantum dots/CoAl-LDH Mott-Schottky heterostructure for enhancing electrochemical properties in supercapacitors. *Chemical Engineering Journal* 2025, 514.[DOI: 10.1016/j.cej.2025.162708]

123. Chaouiki, A.; Chafiq, M.; Ko, Y. G., The art of controlled nanoscale lattices: A review on the self-assembly of colloidal metal-organic framework particles and their multifaceted architectures. *Materials Science & Engineering R-Reports* 2024, 159.[DOI: 10.1016/j.mser.2024.100785]

124. Hu, K.; Li, B.; Tian, Z.; Chen, L. Multiscale Simulation in Fuel Cell and Electrolyzer Systems: A Review of Methods, Applications, and Future Prospects. *Sustainable Engineering Novit* 2025, 1 (1), 5.[DOI: 10.53941/sen.2025.100005]

125. Sun, L. M.; Yuan, Y. S.; Wang, F.; Zhao, Y. L.; Zhan, W. W.; Han, X. G., Selective wet-chemical etching to create TiO2@MOF frame heterostructure for efficient photocatalytic hydrogen evolution. *Nano Energy* 2020, 74.[DOI: 10.1016/j.nanoen.2020.104909]

126. Liu, Y.; Tang, C. S.; Cheng, M.; et al., Polyoxometalate@Metal-Organic Framework Composites as Effective Photocatalysts. *Acs Catalysis* 2021, 11 (21), 13374-96.[DOI: 10.1021/acscatal.1c03866]

127. Jin, Z. C.; Zhu, X. R.; Wang, N. N.; Li, Y. F.; Ju, H. X.; Lei, J. P., Electroactive Metal-Organic Frameworks as Emitters for Self-Enhanced Electrochemiluminescence in Aqueous Medium. *Angewandte Chemie-International Edition* 2020, 59 (26), 10446-50.[PMID: 32196901 DOI: 10.1002/anie.202002713]

128. Mo, R. J.; Chen, S.; Huang, L. Q.; et al., Regulating ion affinity and dehydration of

metal-organic framework sub-nanochannels for high-precision ion separation. *Nature Communications* 2024, 15 (1).[PMID: 38459053 PMCID: PMC10924084 DOI: 10.1038/s41467-024-46378-6]

129. Ma, S. Y.; Han, W. G.; Han, W. L.; Dong, F.; Tang, Z. C., Recent advances and future perspectives in MOF-derived single-atom catalysts and their application: a review. *Journal of Materials Chemistry A* 2023, 11 (7), 3315-63.[PMID: 36594186 DOI: 10.1039/d2mh01067d]

130. Lyu, C.; Ding, Y. M.; Yu, Z. B. A.; et al., Hierarchical Pore Engineering and Single-site Synergy: In situ Construction of Functionalized MOF for Highly Active C-N Coupling. *Acta Chimica Sinica* 2026, 84 (1), 119-28.

131. Zhou, C. Y.; Cui, W.; Cui, S. X.; Li, G. C.; Han, L., MOF-Derived Co(Fe)OOH Slab and Co/MoN Nanosheet-Covered Hollow-Slab for Efficient Overall Water Splitting. *Acs Applied Materials & Interfaces* 2024, 16 (50), 69368-78.[DOI: 10.1021/acsami.4c15634]

132. Farooq, A.; Zafar, F.; Ul Hassan, S.; Nazir, M. S.; Ali, Z.; Ahmad, N.; Ahmad, F., Rational Design of Metal-Organic Framework Hybrids via Metal and Ligand Engineering for Enhanced Oxygen Evolution Reaction Catalysis. *Energy & Fuels* 2025, 39 (50), 23796-804.[DOI: 10.1021/acs.energyfuels.5c04018]

133. Zhang, Z.; Han, L.; Tao, K., MnOx-decorated MOF-derived nickel-cobalt bimetallic phosphide nanosheet arrays for overall water splitting. *Dalton Transactions* 2024, 53 (4), 1757-65.[DOI: 10.1039/D3DT03631F]

134. Ji, L. D.; Wang, J.; Wu, K. B.; Yang, N. J., Tunable Electrochemistry of Electrosynthesized Copper Metal-Organic Frameworks. *Advanced Functional Materials* 2018, 28 (13).[DOI: 10.1002/adfm.201706961]

135. Niu, Q.; Yang, M.; Luan, D.; Li, N. W.; Yu, L.; Lou, X. W., Construction of Ni-Co-Fe Hydr(oxy)oxide@Ni-Co Layered Double Hydroxide Yolk-Shelled Microrods for Enhanced Oxygen Evolution. *Angewandte Chemie-International Edition* 2022, 61 (49).[PMID: 36218244 DOI: 10.1002/anie.202213049]

136. Zhong, L.; Huang, Q.; Ding, J. Y.; et al., Abundant Co-Nx sites onto hollow MOF-Derived nitrogen-doped carbon materials for enhanced oxygen reduction. *Journal*

of Power Sources 2021, 492.[DOI: 10.1016/j.jpowsour.2021.229632]

137. Maji, B.; Nanda, O. P.; Das, N. K.; Badhulika, S., Self-standing 3D-printed gas sensor using molybdenum boride MBene based PCN-224 modified composite for ppb-level detection of formaldehyde at ambient temperature. *Chemical Engineering Journal* 2025, 522.[DOI: 10.1016/j.cej.2025.167092]

138. Peng, B.; She, H.; Wei, Z. H.; et al., Sulfur-doping tunes p-d orbital coupling over asymmetric Zn-Sn dual-atom for boosting CO_2 electroreduction to formate. *Nature Communications* 2025, 16 (1).[DOI: 10.1038/s41467-025-57573-4]

139. Prabhakar, N.; Pramoda, K.; Keri, R. S., Influence on choice of dopants for MOF-based supercapacitor application: Synthesis, properties and electrochemistry. *Journal of Energy Storage* 2025, 140.[DOI: 10.1016/j.est.2025.118986]

140. Liu, Y.; Yuan, Y.; Wang, R.; et al., R. Computational Studies for Aqueous Zinc-Ion Secondary Batteries. *Sustainable Engineering Novit* 2025, 1 (1), 6.[DOI: 10.53941/sen.2025.100006]

141. Li, B. T.; Li, Q.; Yang, S. P.; He, J. J.; Mi, Y. Q.; Du, P. C., Controlled ion-etching synthesis of MOF-derived rattle-type nickel hydroxide nanostructures for enhanced electrochemical performance in supercapacitors. *Electrochimica Acta* 2025, 542.[DOI: 10.1016/j.electacta.2025.147514]

142. Liu, W. T.; Yuan, G. Q.; Jiang, S.; Shi, Y. X.; Pang, H., Two-Dimensional (2D) Conductive Metal-Organic Framework Thin Films: The Preparation and Applications in Electrochemistry. *Chemistry-a European Journal* 2024, 30 (70). DOI: 10.1002/chem.202402747]

143. Al-Aoh, H. A.; Panneerselvam, C.; Alghamdi, A. M.; Alasmari, A.; Mohammedsaleh, Z. M., Recent advances in MXene nanozymes: synthesis, surface modifications, catalytic properties, and their emerging roles in biosensing and therapeutic applications. *Analyst* 2026, 151 (4), 991-1007.[DOI: 10.1039/D5AN01137J]

144. Li, S. C.; Ma, C.; Hou, J. W.; et al., Highly porous metal-organic framework glass design and application for gas separation membranes. *Nature Communications* 2025, 16 (1).[DOI: 10.1038/s41467-025-56295-x]

145. Zhang, M. Y.; Shan, Y. Y.; Kong, Q. Q.; Pang, H., Applications of metal-organic

framework-graphene composite materials in electrochemical energy storage. *Flatchem* 2022, 32.[DOI: 10.1016/j.flatc.2021.100332]

146. Ali, A.; Ahmed, S.; Jiang, W.; Park, G.; Oh, S. J., Harnessing MOF intrinsic properties for enhanced supercapacitor performance. *Current Opinion in Electrochemistry* 2025, 50.[DOI: DOI: 10.1016/j.coelec.2024.101640]

147. Han, D. D.; Wang, P.; Dang, Y. P.; et al., Facile electrochemical conversion strategy for fabricating cobalt-based double metal sulfide nanosheets with high capacity and low electrochemical impedance. *Journal of Alloys and Compounds* 2024, 1007.[DOI: 10.1016/j.jallcom.2024.176401]

148. Yang, X.; Feng, X. T.; Song, D. B.; et al., Alkali-Enhanced Electrochemical Deintercalation of Fluoride Ions on Superlong Lanthanum Metal-Organic Framework Nanowire in Capacitive Deionization. *Acs Sustainable Chemistry & Engineering* 2026, 14 (5), 2406-218.[DOI: 10.1021/acssuschemeng.5c10442]

149. Zang, Y.; Luo, H.; Zhang, H.; Xue, H., Polypyrrole Nanotube-Interconnected NiCo-LDH Nanocages Derived by ZIF-67 for Supercapacitors. *Acs Applied Energy Materials* 2021, 4 (2), 1189-98.[DOI: 10.1021/acsaem.0c02465]

150. Wang, S. J.; Niu, M.; Zheng, J.; et al., Hollow Porous CoP-Carbon Nanocages for Hydrogen Evolution Reactions. *Acs Applied Nano Materials* 2024, 7 (11), 12821-9.[DOI: 10.1021/acsanm.4c01350]

151. Li, Q.; Zhou, J. J.; Zhao, S. H.; et al., Hollow and Hierarchical Cobalt-Metal Organic Framework@CoCr2O4 Microplate Array as a Battery-Type Electrode for High-Performance Hybrid Supercapacitors. *Chemelectrochem* 2020, 7 (2), 437-44.[DOI: 10.1002/celc.201902015]

152. Li, X. R.; Ye, G. Y.; Zhu, W. W.; et al., Directional Construction of Low-Coordination Fe-N3 Coupled with Intrinsic Carbon Defects for High-Efficiency Oxygen Reduction. *Acs Nano* 2024, 18 (35), 24505-14.[DOI: 10.1021/acsnano.4c08695]

153. Husain, A.; Lee, D. E.; Siddiqui, Q. T.; Gunnasegaran, P.; Danish, M.; Jo, W. K., Scalable integration of MOFs, COFs, and MXenes with g-C3N4 for solar H2 generation: A review of energy conversion strategies. I*nternational Journal of Hydrogen Energy* 2025, 150.[DOI: 10.1016/j.ijhydene.2025.150041]

154. Kim, H.; Lah, M. S., Templated and template-free fabrication strategies for zero-dimensional hollow MOF superstructures. *Dalton Transactions* 2017, 46 (19), 6146-58.[DOI: 10.1039/C7DT00389G]

155. Jiang, H.; Chen, Z. C.; Tao, J. Q.; et al., Phase interface manipulation by adjusting atomic ordering in metal-organic framework to facilitate microwave absorption. *Carbon* 2023, 212.[DOI: 10.1016/j.carbon.2023.118107]

156. Liao, X. J.; Fu, H. M.; Yan, T. T.; Lei, J. P., Electroactive metal-organic framework composites: Design and biosensing application. *Biosensors & Bioelectronics* 2019, 146.[DOI: 10.1016/j.bios.2019.111743]

157. Tuan, D. D.; Khiem, C.; Kwon, E.; et al., Hollow porous cobalt oxide nanobox as an enhanced for activating monopersulfate to degrade 2-hydroxybenzoic acid in water. *Chemosphere* 2022, 294.[DOI: 10.1016/j.chemosphere.2021.133441]

158. Tang, X. R.; Li, N.; Pang, H., Metal-organic frameworks-derived metal phosphides for electrochemistry application. *Green Energy & Environment* 2022, 7 (4), 636-61.[DOI: 10.1016/j.gee.2021.08.003]

159. Yang, Y. T.; Yang, Y.; Zhang, X. M.; et al., A hierarchically porous MOF engineered via chelation-etching for high-capacity selective dye adsorption. *Journal of Solid State Chemistry* 2025, 352.[DOI: 10.1016/j.jssc.2025.125609]

160. Hu, A. Q.; Pang, Q. Q.; Tang, C.; et al., Epitaxial Growth and Integration of Insulating Metal-Organic Frameworks in Electrochemistry. *Journal of the American Chemical Society* 2019, 141 (28), 11322-7.[DOI: 10.1021/jacs.9b05869]

161. Li, X. L.; Goh, T. W.; Xiao, C. X.; et al., Synthesis of Monodisperse Palladium Nanoclusters Using Metal-Organic Frameworks as Sacrificial Templates. *Chemnanomat* 2016, 2 (8), 810-5.[DOI: 10.1002/cnma.201600121]

162. Sun, X. Y.; Li, X. C.; Chen, P. G.; Zhu, Y. L., Controllable regulation of defects in nitrogen-doped hollow core-shell magnetoelectric microspheres towards preferable electromagnetic absorption. *Carbon* 2025, 234.[DOI: 10.1016/j.carbon.2024.119963]

163. Xu, S. J.; Huang, Q.; Xue, J. H.; et al., Morphologically Controlled Metal-Organic Framework-Derived FeNi Oxides for Efficient Water Oxidation. *Inorganic Chemistry* 2022, 61 (23), 8909-19.[PMID: 35656800 DOI: 10.1021/acs.inorgchem.2c01035]

164. Liu, H.; Zhang, T. F.; Cui, D.; et al., Defective ferrocene-based metal-organic frameworks for efficient solar-powered water oxidation via the ligand competition and etching effect. *Journal of Colloid and Interface Science* 2024, 657, 664-71.[PMID: 38071815 DOI: 10.1016/j.jcis.2023.12.024]

165. Martín-Jimeno, F. J.; Suárez-García, F.; Paredes, J. I.; et al., A "Nanopore Lithography" Strategy for Synthesizing Hierarchically Micro/Mesoporous Carbons from ZIF-8/Graphene Oxide Hybrids for Electrochemical Energy Storage. *Acs Applied Materials & Interfaces* 2017, 9 (51), 44740-55.[PMID: 29215875 DOI: 10.1021/acsami.7b16567]

166. Threerattanakulpron, N.; Khongtor, N.; Supasitmongkol, S.; Serafin, J.; Chaemchuen, S.; Klomkliang, N., Non-noble metals promoted MOF-derived CuZn catalysts for low-temperature CO_2 hydrogenation to methanol. *Fuel* 2026, 404.[DOI: 10.1016/j.fuel.2025.136274]

167. Mukherjee, P.; Sathiyan, K.; Higashimine, K.; et al., Surface Engineering Approach to Maximize the Potential of Prussian Blue Analog Nanostructures for Electroreduction of CO_2. *Acs Applied Nano Materials* 2026, 9 (9), 4171-83.[DOI: 10.1021/acsanm.5c05533]

168. Wang, M. K.; Zi, Y.; Zhu, J.; Huang, W. C.; Zhang, Z. Z.; Zhang, H., Construction of super-hydrophobic PDMS@MOF@Cu mesh for reduced drag, anti-fouling and self-cleaning towards marine vehicle applications. *Chemical Engineering Journal* 2021, 417.[DOI: 10.1016/j.cej.2021.129265]

169. Li, M. J.; Zhang, G. Y.; Boakye, A.; Chai, H. N.; Qu, L. J.; Zhang, X. J., Recent Advances in Metal-Organic Framework-Based Electrochemical Biosensing Applications. *Frontiers in Bioengineering and Biotechnology* 2021, 9.[PMCID: PMC8716788 PMID: 34976986]

170. Sun, H. Z.; Tang, B. B.; Wu, P. Y., Hydrophilic hollow zeolitic imidazolate framework-8 modified ultrafiltration membranes with significantly enhanced water separation properties. *Journal of Membrane Science* 2018, 551, 283-93.[DOI: 10.1016/j.memsci.2018.01.053]

171. Wang, Y. T.; Wang, Y. H.; Jian, M.; Jiang, Q. T.; Li, X. F., MXene Key Composites:

A New Arena for Gas Sensors. *Nano-Micro Letters* 2024, 16 (1).[PMID: 38842597 PMCID: PMC11156835 DOI: 10.1007/s40820-024-01430-4]

172. Sun, Y.; Wang, Y. X.; Liu, D. M.; et al., MoS_2-Coated MOF-Derived Hollow Heterostructures for Electromagnetic Wave Absorption. *Acs Applied Materials & Interfaces* 2025, 17 (9), 14278-90.[PMID: 39982447 DOI: 10.1021/acsami.4c23019]

173. Lin, Y. H.; Wang, T. S.; Liu, Y. H.; et al., Multi-nanozyme cascade system for boosting colorimetric sensing by selective etching bimetallic MOFs. *Analytica Chimica Acta* 2025, 1353.[PMID: 40221211 DOI: 10.1016/j.aca.2025.343976]

174. Liu, J. W.; Lv, S. Y.; Gong, Y. N.; et al., Water-Etched Approach to Hierarchically Porous Metal-Organic Frameworks with High Stability. *Inorganic Chemistry* 2023, 62 (29), 11611-7.[PMID: 37428154 DOI: 10.1021/acs.inorgchem.3c01351]

175. Liu, S. X.; Lu, J.; Yu, X.; Pang, H.; Zhang, Q.; Park, H. S., Rational design of metal-organic framework-nanoparticle composite electrocatalysts for sustainable nitrogen electrochemistry. *Escience* 2025, 5 (6).[DOI: 10.1016/j.esci.2025.100378]

176. Liu, M. Y.; Li, Q.; Xiao, X. D.; et al., Constructing Co-O-Ce bridge in Mott-Schottky Co/CeO_2 heterojunctions facilitates oxygen electrocatalysis bifunctionality for rechargeable Zn-air batteries. *Journal of Energy Chemistry* 2026, 112, 572-83.[DOI: 10.1016/j.jechem.2025.08.068]

177. Li, H. R.; Wang, H. R.; Li, M. X.; Yan, X.; Li, H. X., Hierarchical MOFs with spatially ordered cascade enzymes for sensitive nitrite immunosensing. *Biosensors & Bioelectronics* 2026, 303.[DOI: 10.1016/j.bios.2026.118550]

178. Liu, C.; Wang, J.; Wan, J. J.; Yu, C. Z., MOF-on-MOF hybrids: Synthesis and applications. *Coordination Chemistry Reviews* 2021, 432.[DOI:10.1016/j.ccr.2020.213743]

179. Yao, C. F.; Hussain, T.; Hu, B.; Yang, J. M.; Liu, J. Y., Mg-MOF-Derived hierarchical porous carbon fiber electrodes for efficient capacitive deionization. *Journal of Electroanalytical Chemistry* 2024, 967.[DOI: 10.1016/j.jelechem.2024.118495]

180. Wang, X.; Zhou, W.; Zhai, S. L.; et al., Metal-Organic Frameworks: Direct Synthesis by Organic Acid-Etching and Reconstruction Disclosure as Oxygen Evolution Electrocatalysts. *Angewandte Chemie-International Edition* 2024, 63 (11).[PMID:

38247990 DOI: 10.1002/anie.202400323]

181. Xu, Y.; Yin, X. B.; He, X. W.; Zhang, Y. K., Electrochemistry and electrochemiluminescence from a redox-active metal-organic framework. *Biosensors & Bioelectronics* 2015, 68, 197-203.[PMID: 25569877 DOI: 10.1016/j.bios.2014.12.031]

182. Wu, C. H.; Chou, L. Y.; Long, L. L.; et al., Structural Control of Uniform MOF-74 Microcrystals for the Study of Adsorption Kinetics. *Acs Applied Materials & Interfaces* 2019, 11 (39), 35820-6.[PMID: 31502435 DOI: 10.1021/acsami.9b13965]

183. Mu, X. Y.; Wang, W. K.; Sun, C. C.; Wang, J. L.; Wang, C. B.; Knez, M., Recent Progress on Conductive Metal-Organic Framework Films. *Advanced Materials Interfaces* 2021, 8 (9).[DOI: 10.1002/admi.202002151]

184. Rossouw, A.; Petrik, L. F.; Nechaev, A. N.; Apel, P. Y., Advancing Functionalized Track-Etched Membranes: Composite and Hybrid Materials through the JINR-South Africa Partnership. *Eurasian Journal of Chemistry* 2025, 119 (3).[DOI: 10.31489/2959-0663/3-25-14]

185. Chai, L. L.; Li, R.; Sun, Y. Z.; Zhou, K.; Pan, J. Q., MOF-derived Carbon-Based Materials for Energy-Related Applications. *Advanced Materials* 2025, 37 (8).[DOI: 10.1002/adma.202413658]

186. Knizikevicius, R., Theoretical investigation of crystallographic orientation effect on the chemical etching rate. *Vacuum* 2017, 136, 101-4.[DOI: 10.1016/j.vacuum.2016.11.028]

187. Sannes, D. K.; Oien-Odegaard, S.; Aunan, E.; Nova, A.; Olsbye, U., Quantification of Linker Defects in UiO-Type Metal-Organic Frameworks. *Chemistry of Materials* 2023, 35 (10), 3793-800.[DOI: 10.1021/acs.chemmater.2c03744]